Lossy Joint Source-Channel Coding for Energy Harvesting Communication Systems

by

Meysam Shahrbaf Motlagh

A thesis
presented to the University of Waterloo
in fulfillment of the
thesis requirement for the degree of
Master of Science
in
Electrical and Computer Engineering

Waterloo, Ontario, Canada, 2014

I hereby declare that I am the sole author of this thesis. This is a true copy of the thesis, including any required final revisions, as accepted by my examiners.

I understand that my thesis may be made electronically available to the public.

Abstract

In this work, we study the problem of lossy joint source-channel coding in an energy harvesting single-user communication system with causal energy arrivals, where the energy storage unit may have leakage. In particular, we investigate the achievable distortion in the transmission of a single source with arbitrary alphabets via an energy harvesting transmitter over a point-to-point channel.

We first establish a lower bound on the achievable distortion. Then, to minimize the distortion we consider an adaptive joint source-channel coding scheme, where the length of channel codewords varies adaptively based on the available battery charge in each communication block. For this scheme, we obtain two coupled equations that determine the mismatch ratio between channel symbols and input symbols as well as the transmission power, both as functions of battery charge.

As examples of continuous and discrete sources, we consider Gaussian and binary sources. In particular, for the Gaussian case, we obtain a closed form expression for the mismatch factor in terms of the *LambertW* function, and show that an increasing transmission power results in a decreasing mismatch factor and vice versa. We also numerically show that when the mismatch factor adaptively changes based on the available charge in the battery, the communication system achieves a smaller distortion compared to that of a constant mismatch factor.

Acknowledgements

First, foremost and solely, I thank God, the most merciful, the all-knowing and the almighty, for everything.

I wish to extend my sincere gratitude to the many people who helped me throughout my journey as a Master's student. I would like to sincerely thank my supervisor, Dr. Patrick Mitran, for his priceless help and support. Dr. Mitran supported me intellectually and financially, challenged me to unleash my potential, gave me the opportunity to present my work and connect to the community. I would like to extend my appreciation to the readers of my thesis, Dr. Mazumdar and Dr. Khandani for reading my thesis and providing their invaluable comments.

Time would fail me to tell how I am indebted to my parents, Akram and Mohammad Bagher, who are simply the best parents one could dream of. May God endow them with best of rewards, for their patience, endurance, and never ending love. I thank my lovely sisters and brother Maryam, Mahboubeh and Mohammad Masoud for filling my empty space in the family, and apologize them for not being with them for this long.

I also appreciate the time I spent and the discussions I had with my friends in our laboratory at the University of Waterloo: Masoud, HamidReza, Ehsan and Nadia.

Dedication

To Him,

who knows everything.

To my lovely parents,

whose unconditional love, support and sacrifice have lit my life.

Table of Contents

List of Tables

List of Figures

Chapter 1

Introduction

1.1 Wireless Sensor Networks

A Wireless Sensor Network (WSN) is a network of spatially distributed sensors which collectively gather and disseminate information (e.g., temperature, vibration, pressure, sound, humidity, etc) across sensing fields. Sensor tasks include sensing, processing (compression) and transmission of data through the network to a destination. As each sensor node can leave or join the network without impacting other nodes, a WSN is typically self-organized and thus plays an important role in unsupervised control systems. Another advanced feature in WSNs is decentralized network management for sensor failure detection. Currently, WSNs are employed in a range of applications such as environmental/earth monitoring [1], health care monitoring [2] and natural disaster relief operation [3]. Each sensor node is often powered by a very small and limited energy storage unit (battery) and therefore has a very short lifetime. Furthermore, in most cases, sensor devices are scattered over remote geographical areas which makes them inaccessible after installation. As a result, regular maintenance and battery replacement for each sensor is impractical, if not impossible. Due to these strict

energy constraints and limitations, the design of energy-efficient WSNs with good lifetime has become a significant challenge. While energy efficiency has always been a concern in WSNs and various energy-efficient protocols have been proposed in the literature for routing [4, 5] and medium access control [6, 7], to develop truly autonomous systems which do not require regular maintenance it is essential to supply a sustainable energy source to sensor devices.

1.2 Energy Harvesting

Energy harvesting (EH), i.e., supplying energy by the harnessing of ambient energy resources such as solar [8], wind [9] and thermal energy [10], is a promising state-of-the-art solution that can significantly improve sensor lifetime. In a typical EH node, the energy required for various sensor tasks is incrementally harvested from the environment and stored during the course of operation. In light of the potential knowledge of future energy arrivals (from renewable energy resources) at the transmitter, two major categories of EH models are considered, namely, online and offline. In the offline regime, it is assumed that time and amount of future energy arrivals are non-causally (deterministic knowledge) known at the transmitter, whereas in the online regime knowledge of future energy arrivals is causally (stochastic knowledge) known at the transmitter. Hence, due to the stochastic nature of renewable energy resources, sensor energy consumption for data transmission task (i.e., transmission power) is a crucial communication resource that must be managed adaptively to achieve reliable performance.

1.3 Bandwidth Mismatch In Source-Channel Coding

The design of robust, simple and optimal joint source-channel coding (JSCC) schemes that can achieve reliable performance for a given channel condition, is a challenge that has been studied in the literature. For instance, in the source-channel transmission of a Gaussian source over a Gaussian channel with one channel use per source symbol, i.e., channel bandwidth is matched to the source bandwidth, uncoded transmission with a linear scaling of the source symbols is known to be optimal [11]. On the other hand, for source-channel coding scheme with a mismatch between source bandwidth and channel bandwidth some achievable schemes have been proposed in the literature [12, 13, 14]. The two-user broadcast channel is an example for which achievable schemes with bandwidth compression (less than one channel use per source symbol) [14], and bandwidth expansion (more than one channel use per source symbol) [13] have been developed. Moreover, some optimal hybrid analogue-digital source-channel coding schemes for a given channel condition have been addressed in [15], where only integer bandwidth compression or expansion has been considered. In addition, sometimes it happens that there are constrains imposed on the source-channel bandwidth mismatch ratio which makes the design process even more complicated. This in turn results in treating the bandwidth mismatch factor as another crucial communication resource whose optimal scheme must be allocated to achieve reliable performance.

1.4 Related Work

Among prior works that consider lossy communication with EH transmitters/receivers are [16, 17, 18, 19, 20, 21, 22]. In [16], the mean squared distortion of the estimated source symbols at the receiver is minimized, where both online and offline EH scenarios are considered and the mismatch factor is always one. In [17], the problem of energy allocation

for data acquisition and transmission in WSNs is studied, and the case of a single sensor as well as the case of multiple sensors are both considered. A similar problem is studied in [18] for the case of a single source with finite battery and data buffer. Another interesting work is [19], where a perturbation-based Lyapunov technique is proposed to obtain an online energy management scheme for source-channel coding of correlated sources. In [20], a Gaussian source is transmitted over a fading channel and the offline minimization of the total distortion over a finite-time horizon is considered. Therein, the optimal compression rate and transmission power policy are found subject to a delay constraint for reconstruction of the source symbols at the receiver. In [21], the problem of uncoded transmission over a fading channel is investigated, and an optimal energy allocation scheme to minimize the total distortion is established.

Communication systems with EH transmitters/receivers have also been studied extensively in the context of lossless transmission. For instance, the offline minimization of the transmission completion time in a single source is considered in [23], where the battery capacity is infinite. This problem has been also extended to the cases of finite battery [24], multiple access channels [23], broadcast channels [25, 26, 27] and fading channels [28]. In another line of work, throughput/sum-throughput maximization is considered for point-to-point channels [29], interference channels [30] and relay channels [31, 32]. A more realistic battery model with energy leakage is also considered in this context [33, 34].

1.5 Thesis Statement and Contributions

In this work, we focus on the design of data transmission policies in EH sensor devices. Specifically, we consider a scenario where a single node continuously senses data from a source and wishes to transmit this data over a point-to-point channel. The harvested energy is stored

in a battery that may leak energy at a rate which depends on the available battery charge. In particular, an ergodic battery charge process can be identified based on a compound Poisson dam storage model in terms of transmission power, battery leakage rate and the energy arrival process. The communication is carried by a joint source-channel coding (JSCC) scheme, where in each communication block a source sequence of fixed length is mapped into a channel codeword whose length depends only on the battery charge. In other words, the mismatch factor between the channel symbols and source symbols is adapted to the battery charge.

We summarize the major contributions of this thesis as follows:

- We formulate and model continuous-time lossy joint source-channel coding in an energy harvesting communication system, where the transmission power and bandwidth mismatch factor, i.e., the length of channel codewords per source symbol, are dynamically adapted to the available battery charge.

- We establish a lower bound on the average distortion and show that in the case of infinite battery capacity and no leakage it is asymptotically achieved with a constant transmission power and a constant mismatch factor.

- Using a calculus of variations technique, we find achievable locally optimal transmission power and mismatch factor policies that minimize the average distortion at the receiver.

- We develop an interesting structural result on the instantaneous distortion. Namely, as long as the battery is not depleted, locally optimal transmission power and mismatch factor policies will adaptively adjust with the battery charge in such a way that the instantaneous distortion is maintained to a constant level.

- For a moderate-size battery, we numerically show that our proposed scheme with an

adaptively varying mismatch factor achieves a smaller average distortion compared to a scheme with a constant mismatch factor.

- For Gaussian and binary sources, we numerically find locally optimal power policies and mismatch factor policies, both as functions of battery charge. With different leakage rates, i.e., zero leakage rate as well as arbitrary non-zero leakage rates, we observe that a good transmission power policy and mismatch factor policy increases and decreases respectively, as the battery charge increases.

1.6 Thesis Organization

The rest of this thesis is organized as follows. In Chapter 2, we study the communication model as well as the EH model. Specifically, the continuous-time formulation of the problem settings as well as modelling of ergodic battery charge process are addressed in Chapter 2. In Chapter 3, we present the problem formulation. A lower bound on the average distortion as well as the achievable scheme of the communication resources are studied in Chapter 4. Some structural results for the instantaneous distortion and the case of Gaussian source are also studied in this Chapter. In Chapter 5, we provide numerical results and simulations. Finally, Chapter 6 concludes this thesis and elaborates on some future research directions.

Chapter 2

Adaptive Resource Allocation for EH Communication Systems When Using A Lossy JSCC Scheme

2.1 Communication Model

We consider the lossy source-channel transmission of a stationary memoryless source with general alphabet (continuous or discrete) over a point-to-point channel. We first assume that the communication is carried over K consecutive blocks of joint source-channel coding (JSCC), where the number of source symbols in each block is fixed, whereas the length of the channel codewords varies from one block to another based on the available charge in the battery. Specifically, during the i^{th} block, $i = 1, ..., K$, a sequence of m independent and identically distributed (i.i.d.) realizations of the source $s_i^m = (s_i[1], s_i[2], ..., s_i[m])$, are mapped to a channel codeword of length n_i, $x_i^{n_i} = (x_i[1], x_i[2], ..., x_i[n_i])$. The input $x_i^{n_i}$

induces a distribution on the channel output $y_i^{n_i} = (y_i[1], y_i[2], ..., y_i[n_i])$, according to the law $\mathbb{P}_Y\left(y_i^{n_i}\right) = \prod_{k=1}^{n_i} \mathbb{P}_{Y|X}(y_i[k]\big|x_i[k])\mathbb{P}_X\left(x_i[k]\right)$, where $\mathbb{P}_{Y|X}\left(y|x\right)$ is the conditional distribution of the stationary and memoryless channel.

We assume that τ is the time duration needed for one symbol to be generated/transmitted. Associated with τ, $\Delta t_s = m \times \tau$ is the time duration to generate m source symbols, and $\Delta t_{c_i} = n_i \times \tau$ is the time duration to transmit a channel codeword of length n_i during the i^{th} block (see Fig. 2.1).

Definition 1. *We define the bandwidth mismatch factor between the i^{th} channel codeword block, with duration Δt_{c_i}, and the source symbol block, with duration Δt_s, as $\kappa(t_{c_i}) = \Delta t_{c_i}/\Delta t_s = n_i/m$ for $i = 1, ..., K$, where $t_{c_i} := \sum_{j=1}^{i} \Delta t_{c_j}$ is the channel output time that we take as the reference time throughout the thesis. Likewise, $\{p(t_{c_i})\}_{i=1}^{K}$ is the average power constraints on the codewords, i.e.,*

$$\frac{1}{n_i}\sum_{j=1}^{n_i}\left|x_i[j]\right|^2 \leq p(t_{c_i}), \quad i = 1, ..., K. \tag{2.1}$$

As demonstrated in Fig. 2.1, the mismatch factor $\kappa(t_{c_i})$ is fixed throughout each block, nevertheless it can change adaptively from one block to another. Similarly, the transmission power $p(t_{c_i})$ can only change from block to block.

The rate-distortion function (i.e., lossy source coding rate) in the i^{th} block, for a source S is given by

$$R_s(D_i) = \inf\ I(\hat{S}; S), \quad i = 1, ..., K, \tag{2.2}$$

where the infimum is taken over all conditional distributions $\mathbb{P}_{\hat{S}|S}$ such that $\mathbb{E}[d(\hat{S}, S)] \leq D_i$ in the i^{th} block, and $I(\hat{S}; S)$ is the mutual information between the estimated symbols $\hat{S}$ and the source symbols S. We assume that for a given source S and distortion measure $d(\hat{s}, s)$

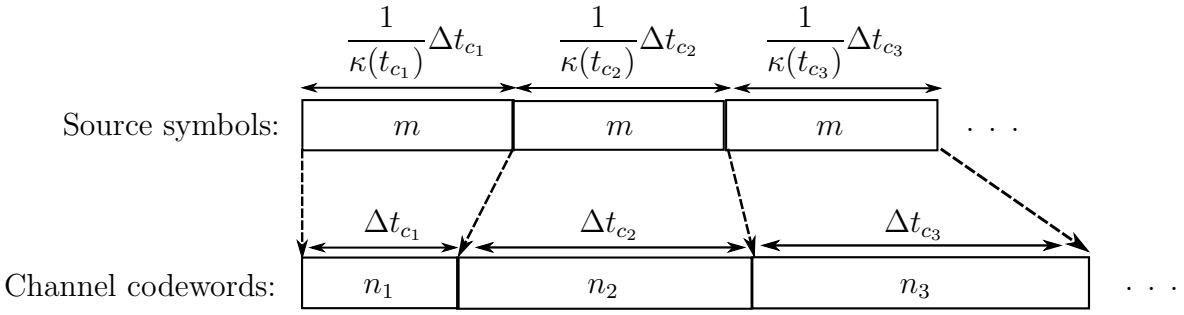

Figure 2.1: Consecutive blocks of JSCC, where m and n_i, $i = 1, ..., K$, are the number of source symbols and length of channel codewords in each block, respectively.

the rate-distortion function $R_s(D)$ has two thresholds $D_{\max}$ and R_s^{th} (where $D_{\max}$ is always finite whereas R_s^{th} could be finite or infinite), such that:

[$S1$] $R_s(D)$ is zero for $D \geq D_{\max}$,

[$S2$] $R_s(D)$ is strictly decreasing, convex and twice continuously differentiable for $0 < D < D_{\max}$, i.e., $R_s'(D) < 0$ and $R_s''(D) > 0$, and continuous at $D = D_{\max}$,

[$S3$] $\lim_{D \downarrow 0} R_s'(D) = -\infty$, and $R_s'(D)$ is finite everywhere else,

[$S4$] $\lim_{D \downarrow 0} R_s(D) = R_s^{\text{th}}$, and $R_s(D)$ is right-continuous at $D = 0$ if R_s^{th} is finite.

An example of a source whose rate-distortion function satisfies these conditions is the Gaussian source $\mathcal{N}(0, \sigma^2)$, where for a squared-error distortion measure $d(\hat{s}, s) = |s - \hat{s}|^2$ its rate-distortion function is given by [35],

$$R_s(D) = \begin{cases} \frac{1}{2} \log \frac{\sigma^2}{D} & 0 < D < \sigma^2 \\ 0 & D \geq \sigma^2. \end{cases} \tag{2.3}$$

Here, we have that $D_{\max} = \sigma^2$ and $R_s^{\text{th}} = \infty$. Another example is a Bernoulli(p) binary source with Hamming distortion $d(\hat{s}, s) = 0$ for $s = \hat{s}$ and $d(\hat{s}, s) = 1$ otherwise. The rate-distortion function is then given by [35],

$$R_s(D) = \begin{cases} H(\mathsf{p}) - h(D) & 0 \leq D < \min\{\mathsf{p}, 1-\mathsf{p}\} \\ 0 & D \geq \min\{\mathsf{p}, 1-\mathsf{p}\}, \end{cases} \tag{2.4}$$

where $H(\mathsf{p})$ is the entropy of the source and

$$h(D) := -D \log_2 D - (1-D) \log_2 (1-D). \tag{2.5}$$

For the binary source, $D_{\max} = \min\{\mathsf{p}, 1-\mathsf{p}\}$ and $R_s^{\text{th}} = H(\mathsf{p})$.

With respect to channel coding in the i^{th} block, the channel coding rate $R_c(p(t_{c_i}))$ is given by

$$R_c(p(t_{c_i})) = \sup I(X;Y), \quad i = 1, ..., K, \tag{2.6}$$

where the supremum is taken over all channel input distributions $\mathbb{P}_X$ that satisfy the power constraint $p(t_{c_i})$ in (2.1) for the i^{th} block. We assume that the channel coding rate $R_c(p)$ has the following properties:

[$C1$] $R_c(p)$ is strictly positive for $p > 0$, zero at $p = 0$ and right-continuous at $p = 0$,

[$C2$] $R_c(p)$ is strictly increasing, concave and twice continuously differentiable for $p > 0$, i.e., $R_c'(p) > 0$ and $R_c''(p) < 0$.

For example, the Shannon rate function $R_c(p) = \frac{1}{2} \log_2(1 + p/N)$, which will be used later in the thesis, satisfies these properties.

We assume that the block lengths m and n_i, $i = 1, ..., K$, are sufficiently large that the rate-distortion function and the channel coding rate have operational significance. Since the

mismatch factor is fixed throughout each JSCC block, source-channel separation holds in each block. Therefore, based on a separate source and channel coding scheme, the relation between source coding rate $R_s(D_i)$ and the channel coding rate $R_c(p(t_{c_i}))$ is given by

$$R_s(D_i) = \kappa(t_{c_i}) R_c(p(t_{c_i})), \quad i = 1, ..., K. \tag{2.7}$$

One should note that by the condition $[S2]$ and continuity of $R_s(D)$ at $D = D_{\max}$, the inverse function $D_i(R_s)$ of the rate-distortion always exists for $0 \leq \kappa(t_{c_i}) R_c(p(t_{c_i})) < R_s^{\text{th}}$ (though in most cases there is no closed-form), and we can compute the distortion $D_i(R_s)$ in the i^{th} block in terms of the transmission power $p(t_{c_i})$ and the mismatch factor $\kappa(t_{c_i})$ using (2.7), i.e., $D_i(R_s) := D(p(t_{c_i}), \kappa(t_{c_i}))$. Moreover, if R_s^{th} is finite then the distortion is $D(p(t_{c_i}), \kappa(t_{c_i})) = 0$ for pairs $p(t_{c_i}), \kappa(t_{c_i})$ such that $\kappa(t_{c_i}) R_c(p(t_{c_i})) \geq R_s^{\text{th}}$.

From the definition of the mismatch factor and Fig. 2.1, we directly obtain

$$K \times \Delta t_s = \sum_{i=1}^{K} \frac{1}{\kappa(t_{c_i})} \Delta t_{c_i}. \tag{2.8}$$

Eq. (2.8) can be used to recast the average distortion in terms of the output reference time t_c. Specifically, the total average distortion per source symbol over K blocks can be written as

$$D_{\text{avg}} := \frac{1}{K \Delta t_s} \sum_{i=1}^{K} D(p(t_{c_i}), \kappa(t_{c_i})) \Delta t_s \tag{2.9}$$

$$= \frac{1}{K \Delta t_s} \sum_{i=1}^{K} D(p(t_{c_i}), \kappa(t_{c_i})) \frac{1}{\kappa(t_{c_i})} \Delta t_{c_i}. \tag{2.10}$$

2.2 Continuous-Time Model

As a practical assumption, we suppose that both the source and the channel block times, Δt_s and Δt_{c_i} respectively, are small compared to the battery dynamics. Hence, we develop a continuous-time model in the asymptotic regimes based on (2.8) and (2.10), and let K grow so that

$$T_s := K\Delta t_s$$
$$T_c := \sum_{i=1}^{K} \Delta t_{c_i},$$

where the terms T_s and T_c have fixed values as $\Delta t_s \to 0$, $\Delta t_{c_i} \to 0$ and $K \to \infty$. In the limit of $\Delta t_s \to 0$, $\Delta t_{c_i} \to 0$ and $K \to \infty$, (2.8) is a Reimann sum and thus the continuous-time limit takes the following form

$$T_s = \int_0^{T_c} \frac{1}{\kappa(t_c)} dt_c. \tag{2.11}$$

We define

$$\rho(T_c) := \frac{T_s}{T_c} = \frac{1}{T_c} \int_0^{T_c} \frac{1}{\kappa(t_c)} dt_c. \tag{2.12}$$

In this thesis, we are interested in infinite-time horizon communication and long-term average distortion. We thus let the transmission time become asymptotically large, i.e., $T_c \to \infty$. If $\lim_{T_c\to\infty} \rho(T_c) > 1$ or $\lim_{T_c\to\infty} \rho(T_c) < 1$, the backlog in either the source symbols queue or the transmission of channel codewords tends to infinity. Thus, the joint source-channel communication system is asymptotically stable if $\lim_{T_c\to\infty} \rho(T_c) = \lim_{T_c\to\infty} T_s/T_c = 1$. Therefore, from (2.12) for an asymptotically stable joint source-channel communication system we

require that,

$$\lim_{T_c\to\infty}\frac{1}{T_c}\int_0^{T_c}\frac{1}{\kappa(t_c)}dt_c = 1. \tag{2.13}$$

Hence, we rewrite the continuous-time limit of (2.10) as

$$\begin{aligned} D_{\text{avg}} &= \lim_{T_c\to\infty}\frac{1}{T_s}\int_0^{T_c} D(p(t_c),\kappa(t_c))\frac{1}{\kappa(t_c)}dt_c \\ &= \lim_{T_c\to\infty}\frac{1}{T_c}\int_0^{T_c} D(p(t_c),\kappa(t_c))\frac{1}{\kappa(t_c)}dt_c, \end{aligned} \tag{2.14}$$

where (2.14) follows from the fact that $\lim_{T_c\to\infty} T_s/T_c = 1$.

2.3 Storage Model

We assume that the energy arrival times and amounts to the battery are not known at the transmitter. However, their statistical properties are known. Therefore, the instantaneous energy of the battery is a stochastic process that can be characterized based on the statistics of energy arrivals. Let $\{E_i\}_{i=1}^{\infty}$, denote the size of the energy packets arriving to the battery at time instants $\{T_i\}_{i=1}^{\infty}$, where $E_i > 0$ and $T_1 < T_2 < \dots$. We assume that energy packets are i.i.d. with the tail distribution function denoted by $B(z) = \mathbb{P}[E > z]$, and the corresponding arrival times are a homogeneous Poisson point process. Specifically, the inter-arrival times are i.i.d. and exponentially distributed with parameter δ, i.e., $\Delta T_n := T_{n+1} - T_n \sim Exp(\delta)$. The total harvested energy at the transmitter up to the time t, $\{A(t) : t \geq 0\}$ is thus a compound Poisson process given by

$$A(t) = \sum_{n\in\mathbb{N}} E_n \mathbb{1}_{\{T_n<t\}}. \tag{2.15}$$

We assume that the capacity of the battery L is finite, that is, $L < \infty$. Furthermore, we assume that the battery is imperfect in the sense that it may leak energy over time at a rate which depends only on the current battery charge $Z(t)$, and is denoted by $\ell(t)$ at time t. Also, it is clear that there is no leakage when the battery is depleted.

The instantaneous battery charge at time t, $\{Z(t) : t \geq 0\}$ is therefore a stochastic process described by

$$Z(t) = z_0 + A(t) - \int_{0^+}^{t} \Big(p\,(s) + \ell(s)\Big) ds - R(t), \tag{2.16}$$

where $z_0 = Z(t)|_{t=0}$ is the initial battery charge and $R(t)$ is a non-decreasing and continuous-time *reflection* process with $R(t)|_{t=0} = 0$, that only increases over the set $\{t : Z(t) = L\}$ [36]. The reflection process accounts for the excess energy arrivals that overflow the battery capacity and ensures that even for large energy packet arrivals the storage process satisfies its capacity limit at all times, i.e., $Z(t) \in [0, L]$. Furthermore, $p(t)+\ell(t)$ is the instantaneous battery depletion rate which depends on time only through $Z(t)$, i.e., $p(t)+\ell(t) = p\,(Z(t))+\ell\,(Z(t))$. Likewise, the instantaneous mismatch factor $\kappa(t)$ is modulated by the battery charge $Z(t)$, where $\kappa(t) = \kappa(Z(t))$. More specifically, since $p(t)$, $\ell(t)$ and $\kappa(t)$ depend on t only through the battery charge $Z(t)$, with slight abuse of notation we denote by $p(z)$, $\ell(z)$ and $\kappa(z)$ the explicit dependence of these on z. In the rest of this thesis, we refer to $p(z)$ and $\kappa(z)$ as the power policy and mismatch factor policy. The storage process $Z(t)$ can then be viewed as a continuous-time Markov process, where the state space of the process is the finite interval $[0, L]$. We impose the following conditions on the feasible set of power policies and leakage rates

- $\forall z \in (0, L],\ p(z) > 0$, and $p(z)\big|_{z=0} = 0$,
- $\sup_{0<z\leq L} p(z) < \infty$,

- $\sup_{0<z\leq L} \ell(z) < \infty$, and $\ell(z)\big|_{z=0} = 0$.

The first condition is to avoid a reserve of energy in the battery that can never be consumed by transmission, and thus effectively reduces the usable energy stored in the battery. The second condition reflects the fact that instant depletion of an amount of energy $\Delta E > 0$ is not allowed. With these conditions on $p(z)$ and $\ell(z)$, $Z(t)$ becomes irreducible in the sense that there is only one single communicating class in the state space. For an irreducible Markov chain, either all states are recurrent or all states are transient. Since, every irreducible Markov chain with a closed and bounded state space is positive recurrent, the storage process $Z(t)$ is thus positive recurrent.

We define $\tilde{\pi}_{T_c}(z)$ as the empirical distribution function of the storage process with respect to the reference time, i.e.,

$$\tilde{\pi}_{T_c}(z) := \frac{1}{T_c} \int_0^{T_c} \mathbb{1}_{\{Z(t_c)\leq z\}} dt_c. \tag{2.17}$$

By the strong law of large numbers, as $T_c \to \infty$, $\tilde{\pi}_{T_c}(z)$ converges to the stationary probability measure of the storage process denoted by $\pi(z)$, almost surely for every value of z. The following theorem states the ergodicity condition for the storage process $Z(t)$ [37], where we recall that the inter-arrival times are i.i.d. and exponentially distributed with parameter δ, i.e., $T_{n+1} - T_n \sim Exp(\delta)$.

Theorem 1. *For $L < \infty$, the storage process $Z(t)$ is positive recurrent and there exists a unique stationary probability measure $\pi(z) = \mathbb{P}[Z(t) \leq z]$, which may have an atom $\pi_0 := \pi(z)|_{z=0} \geq 0$, and is absolutely continuous on $(0, L]$ such that*

$$\pi(z) = \pi_0 + \int_{0^+}^{z} f(u)du, \tag{2.18}$$

where $f(z)$ is the absolutely continuous part of the probability measure of the storage process

for $z > 0$. Moreover,

$$f(z)\left(p(z)+\ell(z)\right) = \delta\pi_0 B(z) + \delta\int_{0^+}^{z} B(z-u)f(u)du. \tag{2.19}$$

Remark 1. *From* (2.17)*, π_0 is the fraction of time that the battery remains discharged.*

Remark 2. *Equation* (2.19) *is the equilibrium condition between the rate of down-crossing $f(z)(p(z)+\ell(z))$ and the rate of up-crossing $\delta\pi_0 B(z) + \delta\int_{0^+}^{z} B(z-u)f(u)du$ at a threshold $Z = z$.*

We now assume that the packets of energy are exponentially distributed with parameter λ, i.e., $B(z) = \exp(-\lambda z)$. Therefore, (2.19) reduces to

$$f(z)\left(p(z)+\ell(z)\right) = \delta e^{-\lambda z}\left(\pi_0 + \int_{0^+}^{z} e^{\lambda u} f(u)du\right). \tag{2.20}$$

Chapter 3

Problem Formulation

In this chapter, we formulate a non-linear optimization problem whose solution determines the structure of a locally optimal achievable scheme for transmission power policy and mismatch factor policy.

Since, $\pi(z)$ is a probability measure we have

$$\int_0^L \pi(dz) = \pi_0 + \int_{0^+}^L f(z)dz = 1. \tag{3.1}$$

By combining (2.13) and (2.18), we also obtain the following constraint on the mismatch factor

$$\lim_{T_c\to\infty} \frac{1}{T_c}\int_0^{T_c} \frac{1}{\kappa(Z(t_c))}dt_c = \mathbb{E}_\pi\left[\frac{1}{\kappa(z)}\right] \qquad a.s. \tag{3.2}$$

$$= \frac{\pi_0}{\kappa_0} + \int_{0^+}^L \frac{f(z)}{\kappa(z)}dz \tag{3.3}$$

$$= 1, \tag{3.4}$$

where $\kappa_0 := \kappa(z)|_{z=0}$ is the number of channel uses per source symbol when the battery is exhausted. Similarly, we apply the ergodicity argument to the distortion function in (2.14). We first rewrite D_{avg} from (2.14) as

$$D_{\text{avg}} = \lim_{T_c \to \infty} \frac{1}{T_c} \int_0^{T_c} D\Big(p\left(Z\left(t_c\right)\right), \kappa\left(Z\left(t_c\right)\right)\Big) \frac{1}{\kappa\left(Z\left(t_c\right)\right)} dt_c. \tag{3.5}$$

Due to the ergodicity of the storage process $Z(t_c)$, we obtain

$$\begin{aligned} D_{\text{avg}} &= \int_0^L D\left(p(z), \kappa(z)\right) \frac{1}{\kappa(z)} \pi(dz) \qquad a.s. && (3.6)\\ &= \pi_0 D^\dagger(p(0), \kappa_0) + \int_{0^+}^L D^\dagger\left(p(z), \kappa(z)\right) f(z) dz && (3.7)\\ &= \mathbb{E}_\pi \left[D^\dagger \left(p(Z), \frac{1}{\kappa(Z)} \right) \right], && (3.8) \end{aligned}$$

where

$$D^\dagger \left(p(z), \frac{1}{\kappa(z)} \right) := D(p(z), \kappa(z)) \frac{1}{\kappa(z)}. \tag{3.9}$$

We now wish to find the optimal transmission power policy $p(z)$ and mismatch factor policy $\kappa(z)$ such that the distortion at the receiver is minimized. More specifically, we want to minimize (3.7) subject to the constraints in (2.20), (3.1) and (3.4), i.e.,

$$\begin{aligned} \inf_{f(z), \pi_0, \kappa(z), \kappa_0} \quad & \pi_0 D^\dagger(p(0), \kappa_0) + \int_{0^+}^L D^\dagger\left(p(z), \kappa(z)\right) f(z) dz && (3.10)\\ \text{subject to: } & f(z)\left(p(z) + \ell(z)\right) = \delta e^{-\lambda z} \Big(\pi_0 + \int_{0^+}^L e^{\lambda u} f(u) du \Big) && (3.11)\\ & \pi_0 + \int_{0^+}^L f(z) dz = 1 && (3.12)\\ & \frac{\pi_0}{\kappa_0} + \int_{0^+}^L \frac{f(z)}{\kappa(z)} dz = 1 && (3.13)\\ & f(z) \geq 0, \quad \pi_0 \geq 0, \quad \kappa(z) > 0, \quad \kappa_0 > 0, && (3.14) \end{aligned}$$

where the strict inequalities $\kappa(z) > 0$ and $\kappa_0 > 0$ are implied by (3.13). We note that for a given $f(z)$, $p(z)$ can be calculated directly using (3.11).

From (3.13), we see that the inverse mismatch factor $1/\kappa(z)$ must average to one. Hence, a feasible mismatch factor policy $\kappa(z)$ must balance large mismatch factors (which help reduce the instantaneous distortion) for some battery charge levels z, with small mismatch factors for other battery charge levels to maintain this average constraint. One can thus view the mismatch factor $\kappa(z)$ as a limited resource in the sense that instantaneous deviations from one are permissible only in as much as they are balanced such that the average constraint in (3.13) is assured.

Similarly, the transmitter cannot consume more energy than what is stored in the battery, which itself is replenished at a maximum rate of δ/λ (ignoring the energy that is lost due to overflow). Thus, similar to the mismatch factor, one can view the transmission power $p(z)$ as a limited resource in the sense that a large transmission power for some battery charge levels z must as well be balanced by a small transmission power for other battery charge levels.

Chapter 4

Lower Bound on the Total Average Distortion and Achievable Schemes

4.1 Distortion Lower Bound

In this chapter, we derive a distortion lower bound using Jensen's inequality and find certain conditions under which the lower bound is achieved with a proper allocation of transmission power and mismatch factor. Thereafter, we identify the structure of a locally optimal achievable scheme for $p(z)$ and $\kappa(z)$. Furthermore, we study some structural results on the instantaneous distortion and the case of Gaussian source.

4.1.1 Finite Battery Capacity

We first note that for any power policy $p(z)$, when the battery capacity is finite, the following upper bound on the average transmission power can be obtained:

$$\begin{aligned}
\mathbb{E}_\pi\left[p(Z)\right] &= \int_0^L p(z)\pi(dz) \\
&= \int_{0^+}^L p(z)f(z)dz \\
&\overset{(a)}{=} \delta\int_{0^+}^L e^{-\lambda z}\left(\pi_0 + \int_{0^+}^z e^{\lambda u}f(u)du\right)dz - \int_{0^+}^L f(z)\ell(z)dz \\
&\overset{(b)}{=} -\frac{\delta}{\lambda}e^{-\lambda z}\left(\pi_0 + \int_{0^+}^z e^{\lambda u}f(u)du\right)\Big|_{0^+}^L + \frac{\delta}{\lambda}\int_{0^+}^L f(z)dz - \int_{0^+}^L f(z)\ell(z)dz \\
&= \frac{\delta}{\lambda}\left[-e^{-\lambda L}\left(\pi_0 + \int_{0^+}^L e^{\lambda u}f(u)du\right) + \pi_0 + \int_{0^+}^L\left(1-\frac{\lambda}{\delta}\ell(z)\right)f(z)dz\right] \\
&\overset{(c)}{=} \frac{\delta}{\lambda}\left[-e^{-\lambda L}\int_0^L e^{\lambda u}\pi(du) + \pi_0\left(1-\frac{\lambda}{\delta}\ell(0)\right) + \int_{0^+}^L\left(1-\frac{\lambda}{\delta}\ell(z)\right)f(z)dz\right] \\
&= \frac{\delta}{\lambda}\left[\int_0^L\left(1-\frac{\lambda}{\delta}\ell(z)-\frac{e^{\lambda z}}{e^{\lambda L}}\right)\pi(dz)\right] \\
&\leq \frac{\delta}{\lambda}\sup_{z\in[0,L]}\left(1-\frac{\lambda}{\delta}\ell(z)-\frac{e^{\lambda z}}{e^{\lambda L}}\right) \\
&= \frac{\delta}{\lambda}\left(1-e^{-\lambda L}\right), \qquad (4.1)
\end{aligned}$$

where (a) follows from (2.19), (b) follows by integrating the first integral by parts and (c) follows from the fact that $\pi_0 = \pi_0\left(1-\frac{\lambda}{\delta}\ell(0)\right)$. One should note that the upper bound in (4.1) is potentially a looser bound compared to the case where the leakage is zero. We now find a lower bound on the objective function $\mathbb{E}_\pi[D^\dagger(p(Z), 1/\kappa(Z))]$, based on the upper bound in (4.1) and the following convexity lemma.

Lemma 1. *The function $D^\dagger(p(z), q(z))$ is jointly convex over the pair $p(z)$ and $q(z)$, where $q(z) := 1/\kappa(z)$.*

Proof. See Appendix A. □

Based on Lemma 1 as well as Jensen's inequality, we establish a distortion lower bound as below

$$\begin{aligned}\mathbb{E}_\pi\left[D^\dagger\left(p(Z),\frac{1}{\kappa(Z)}\right)\right] &\geq D^\dagger\left(\mathbb{E}_\pi\left[p(Z)\right],\mathbb{E}_\pi\left[\frac{1}{\kappa(Z)}\right]\right) &(4.2)\\ &\geq D^\dagger\left(\frac{\delta}{\lambda}\left(1-e^{-\lambda L}\right),1\right) &(4.3)\\ &:= D_{\mathrm{LB}},\end{aligned}$$

where (4.3) follows from (4.1) and the fact that the distortion function $D^\dagger$ is a non-increasing function of $p(z)$, and further recalling that $\mathbb{E}_\pi[1/\kappa(Z)] = 1$ from (3.4). The lower bound in (4.3) holds for any transmission power $p(z)$ and mismatch factor $\kappa(z)$ that satisfies (3.13) and (3.14).

4.1.2 Infinite Battery Capacity

When the capacity of the battery is infinite, i.e., $L \to \infty$, and therefore the chance of battery overflow is zero, for any ergodic power policy $p(z)$, we obtain the following upper bound,

$$\begin{aligned}\mathbb{E}_\pi\left[p(Z)\right] &= \delta\int_{0^+}^{\infty} e^{-\lambda z}\left(\pi_0+\int_{0^+}^{z} e^{\lambda u}f(u)du\right)dz-\int_{0^+}^{\infty} f(z)\ell(z)dz\\ &= \frac{\delta}{\lambda}\pi_0+\delta\int_{0^+}^{\infty} e^{-\lambda z}\left(\int_{0^+}^{z} e^{\lambda u}f(u)du\right)dz-\int_{0^+}^{\infty} f(z)\ell(z)dz\\ &\overset{\text{(a)}}{=} \frac{\delta}{\lambda}\pi_0+\delta\int_{0^+}^{\infty} e^{\lambda u}f(u)\left(\int_{u}^{\infty} e^{-\lambda z}dz\right)du-\int_{0^+}^{\infty} f(z)\ell(z)dz\\ &= \frac{\delta}{\lambda}\left[\int_{0}^{\infty}\left(1-\frac{\lambda}{\delta}\ell(z)\right)\pi(dz)\right]\\ &\leq \frac{\delta}{\lambda}\sup_{z\in[0,\infty)}\left(1-\frac{\lambda}{\delta}\ell(z)\right)\end{aligned}$$

$$= \frac{\delta}{\lambda}, \tag{4.4}$$

where in (a) we changed the order of the double integral. Consequently the lower bound in (4.3) simplifies to

$$\mathbb{E}_\pi \left[D^\dagger \left(p(Z), \frac{1}{\kappa(Z)} \right) \right] \geq D^\dagger \left(\frac{\delta}{\lambda}, 1 \right). \tag{4.5}$$

One should note that if the leakage rate is zero, every ergodic power policy $p(z)$ is such that $\mathbb{E}_\pi [p(Z)] = \delta/\lambda$. This suggests that in the infinite battery capacity case with no leakage, separate source and channel coding with a constant mismatch factor $\kappa(z) = 1$ may be optimal. More precisely, consider the following choice of power policy

$$p^\star(z) = \frac{\delta}{\lambda} + \epsilon, \quad z > 0, \tag{4.6}$$

with $p^\star(0) = 0$, and $\epsilon > 0$ is a small positive number that ensures the storage process is positive recurrent, and choose $\kappa^\star(z) = 1$ for $z \geq 0$. Then,

$$\mathbb{E}_\pi [p^\star(Z)] = \left(\frac{\delta}{\lambda} + \epsilon \right) (1 - \pi_0), \tag{4.7}$$

and since we must have $\mathbb{E}_\pi[p^\star(z)] = \delta/\lambda$, then

$$1 - \pi_0 = \frac{\delta/\lambda}{\delta/\lambda + \epsilon}. \tag{4.8}$$

In particular, we then compute the total average distortion of this scheme as

$$\mathbb{E}_\pi \left[D^\dagger \left(p^\star(Z), \frac{1}{\kappa^\star(Z)} \right) \right] = (1 - \pi_0) D^\dagger \left(\frac{\delta}{\lambda} + \epsilon, 1 \right) + \pi_0 D_{\max}. \tag{4.9}$$

As $\epsilon \to 0$ the atom π_0 tends to zero from (4.8) and the lower bound in (4.5) is thus asymptotically achieved.

4.2 Locally Optimal Achievable Scheme

The two functions $p(z)$ and $\kappa(z)$ are the policies that we wish to design in this subsection to manage the limited resources of the system in such a way that the average distortion in (3.10) is minimized. To this end, we use a calculus of variations technique which provides necessary conditions for a local and therefore global optimal solution to our optimization problem.

4.2.1 Calculus of Variations Set Up

We define $f^\epsilon(z)$ and $1/\kappa^\epsilon(z)$ as a perturbed density function and perturbation of the inverse mismatch factor, respectively, i.e.,

$$f^\epsilon(z) := f(z) + \epsilon h(z), \tag{4.10}$$

$$\frac{1}{\kappa^\epsilon(z)} := \frac{1}{\kappa(z)} + \epsilon g(z), \tag{4.11}$$

where $h(z)$ and $g(z)$ are continuous and bounded perturbation functions on $(0, L]$, with $h(0^+) = h(L) = 0$ and $g(0^+) = g(L) = 0$. For sufficiently small $\epsilon > 0$, the perturbed density function $f^\epsilon(z)$ satisfies (3.12) only if

$$\pi_0 + \int_{0^+}^{L} f^\epsilon(z)dz = \pi_0 + \int_{0^+}^{L} f(z)dz + \epsilon \int_{0^+}^{L} h(z)dz \tag{4.12}$$

$$= 1, \tag{4.13}$$

which due to (3.1) is true for all $\epsilon > 0$ iff

$$\int_{0^+}^{L} h(z)dz = 0. \tag{4.14}$$

In addition, from (3.13) we derive the two following conditions

$$\frac{\pi_0}{\kappa_0} + \int_{0^+}^{L} \frac{f(z)}{\kappa^{\epsilon}(z)}dz = 1, \tag{4.15}$$

$$\frac{\pi_0}{\kappa_0} + \int_{0^+}^{L} \frac{f^{\epsilon}(z)}{\kappa(z)}dz = 1. \tag{4.16}$$

We simplify (4.15) using (4.11) as follows

$$\frac{\pi_0}{\kappa_0} + \int_{0^+}^{L} \left(\frac{1}{\kappa(z)} + \epsilon g(z)\right) f(z)dz = \frac{\pi_0}{\kappa_0} + \int_{0^+}^{L} \frac{f(z)}{\kappa(z)}dz + \epsilon \int_{0^+}^{L} g(z)f(z)dz \tag{4.17}$$

$$= 1. \tag{4.18}$$

Similarly, we simplify (4.16) using (4.10) as

$$\frac{\pi_0}{\kappa_0} + \int_{0^+}^{L} \frac{f^{\epsilon}(z)}{\kappa(z)}dz = \frac{\pi_0}{\kappa_0} + \int_{0^+}^{L} \frac{f(z)}{\kappa(z)}dz + \epsilon \int_{0^+}^{L} \frac{h(z)}{\kappa(z)}dz \tag{4.19}$$

$$= 1. \tag{4.20}$$

Thus, analogous to the constraint in (4.14), both (4.17) and (4.19) are true for sufficiently small ϵ iff the perturbation functions also satisfy the following constraints

$$\int_{0^+}^{L} g(z)f(z)dz = 0 \tag{4.21}$$

$$\int_{0^+}^{L} \frac{h(z)}{\kappa(z)}dz = 0. \tag{4.22}$$

4.2.2 Necessary Conditions for Optimality of $p(z)$ and $\kappa(z)$

For sufficiently small ϵ, two necessary conditions for a local and therefore a global optimal solution to the optimization problem in (3.10)-(3.14) are

$$\mathbb{E}_{\pi^\epsilon}\left[D^\dagger\left(p^\epsilon(Z),\frac{1}{\kappa(Z)}\right)\right] \geq \mathbb{E}_{\pi}\left[D^\dagger\left(p(Z),\frac{1}{\kappa(Z)}\right)\right], \tag{4.23}$$

$$\mathbb{E}_{\pi}\left[D^\dagger\left(p(Z),\frac{1}{\kappa^\epsilon(Z)}\right)\right] \geq \mathbb{E}_{\pi}\left[D^\dagger\left(p(Z),\frac{1}{\kappa(Z)}\right)\right], \tag{4.24}$$

where $\mathbb{E}_{\pi^\epsilon}$ is the expectation with respect to the probability measure with the perturbed density function $f^\epsilon(z)$, (see (4.10)).

We now expand the l.h.s of (4.23) as below

$$\mathbb{E}_{\pi^\epsilon}\left[D^\dagger\left(p^\epsilon(Z),\frac{1}{\kappa(Z)}\right)\right] = \pi_0 D^\dagger\left(p(0),\kappa_0\right) + \int_{0^+}^{L} D^\dagger(p^\epsilon(z),\kappa(z))f^\epsilon(z)dz. \tag{4.25}$$

We then use (3.11) to compute $p^\epsilon(z)$ as follows

$$p^\epsilon(z) = \delta e^{-\lambda z}\frac{\left(\pi_0 + \int_{0^+}^{z} e^{\lambda u} f^\epsilon(u)du\right)}{f^\epsilon(z)} - \ell(z) \tag{4.26}$$

$$= \delta e^{-\lambda z}\frac{\left(\pi_0 + \int_{0^+}^{z} e^{\lambda u} f(u)du + \epsilon\int_{0^+}^{z} e^{\lambda u} h(u)du\right)}{f(z)+\epsilon h(z)} - \ell(z). \tag{4.27}$$

We also compute the derivative of $p^\epsilon(z)$ with respect to ϵ as follows

$$\frac{dp^\epsilon(z)}{d\epsilon}\Big|_{\epsilon=0} = \delta e^{-\lambda z}\frac{\int_{0^+}^{z} e^{\lambda u}h(u)du}{f(z)} - \frac{h(z)}{f(z)}p(z). \tag{4.28}$$

Based on (4.28), we expand $D(p^\epsilon(z),\kappa(z))$ to first order in ϵ, i.e.,

$$D(p^\epsilon(z),\kappa(z)) = D(p(z),\kappa(z)) + \epsilon\frac{\partial D(p(z),\kappa(z))}{\partial p(z)}\frac{dp^\epsilon(z)}{d\epsilon}\Big|_{\epsilon=0} + O(\epsilon^2). \tag{4.29}$$

Substituting $D(p^\epsilon(z),\kappa(z))$ and $f^\epsilon(z)$ into (4.25) results in

$$\mathbb{E}_{\pi^\epsilon}\left[D^\dagger\left(p^\epsilon(Z),\frac{1}{\kappa(Z)}\right)\right] \tag{4.30}$$
$$= \pi_0 D^\dagger(p(0),\kappa_0) + \int_{0^+}^{L}\left(D(p(z),\kappa(z)) + \epsilon\frac{\partial D(p(z),\kappa(z))}{\partial p(z)}\frac{dp^\epsilon(z)}{d\epsilon}\Big|_{\epsilon=0}\right)\times\left(\frac{f(z)+\epsilon h(z)}{\kappa(z)}\right)dz$$
$$= \mathbb{E}_{\pi}\left[D^\dagger\left(p(Z),\frac{1}{\kappa(Z)}\right)\right]$$
$$+\epsilon\int_{0^+}^{L}\left(D(p(z),\kappa(z))\frac{h(z)}{\kappa(z)} + \frac{\partial D(p(z),\kappa(z))}{\partial p(z)}\frac{dp^\epsilon(z)}{d\epsilon}\Big|_{\epsilon=0}\frac{f(z)}{\kappa(z)}\right)dz, \tag{4.31}$$

where we have neglected the higher order terms of ϵ (i.e., $O(\epsilon^2)$). By substituting (4.31) into (4.23), we establish the following necessary condition for a local and therefore a global optimal power policy $p(z)$

$$\int_{0^+}^{L} D(p(z),\kappa(z))\frac{h(z)}{\kappa(z)}dz - \int_{0^+}^{L}\frac{\partial D(p(z),\kappa(z))}{\partial p(z)}\frac{h(z)}{\kappa(z)}p(z)dz$$
$$+\delta\left[\int_{0^+}^{L}\frac{\partial D(p(z),\kappa(z))}{\partial p(z)}\frac{1}{\kappa(z)}\left(\int_{0^+}^{z}e^{-\lambda(z-u)}h(u)du\right)dz\right] = 0. \tag{4.32}$$

By changing the order of the double integral in the third term of (4.32) we obtain

$$\int_{0^+}^{L} h(z)\left(\delta\int_{z}^{L}\frac{\partial D(p(u),\kappa(u))}{\partial p(u)}\frac{e^{-\lambda(u-z)}}{\kappa(u)}du + \frac{D(p(z),\kappa(z))}{\kappa(z)} - \frac{\partial D(p(z),\kappa(z))}{\partial p(z)}\frac{p(z)}{\kappa(z)}\right)dz = 0. \tag{4.33}$$

Equation (4.33) holds for all perturbation functions $h(z)$, that satisfy (4.14) and (4.22). We can thus rewrite (4.33) as follows

$$\int_{0^+}^{L} h(z)\Bigg(\delta\int_{z}^{L}\frac{\partial D(p(u),\kappa(u))}{\partial p(u)}\frac{e^{-\lambda(u-z)}}{\kappa(u)}du + \frac{D(p(z),\kappa(z))}{\kappa(z)} - \frac{\partial D(p(z),\kappa(z))}{\partial p(z)}\frac{p(z)}{\kappa(z)}$$

$$+\frac{C_1}{\kappa(z)}+C_2\Bigg)dz=0, \quad (4.34)$$

where C_1 and C_2 are two free constants. Therefore, based on the fundamental lemma of the calculus of variations we derive the following equation

$$\delta e^{\lambda z}\kappa(z)\int_z^L \frac{\partial D(p(u),\kappa(u))}{\partial p(u)}\frac{e^{-\lambda u}}{\kappa(u)}du + D(p(z),\kappa(z)) - \frac{\partial D(p(z),\kappa(z))}{\partial p(z)}p(z) + C_1 + C_2\kappa(z) = 0. \quad (4.35)$$

Eq. (4.35) is an integro-differential equation involving $p(z)$ and $\kappa(z)$. However, by multiplying both sides of (4.35) by $e^{-\lambda z}$ and taking derivative of both sides with respect to z and performing further simplifications, we derive a first order non-linear autonomous ordinary differential equation (ODE) equivalent to (4.35) as follows,

$$\begin{aligned} &D(p(z),\kappa(z))\left(\lambda\kappa(z)+\kappa'(z)\right) + \frac{\partial D(p(z),\kappa(z))}{\partial p(z)}\left(\delta\kappa(z) - p(z)\left(\lambda\kappa(z)+\kappa'(z)\right)\right) \\ &- \kappa'(z)\kappa(z)\frac{\partial D(p(z),\kappa(z))}{\partial \kappa(z)} + p(z)\kappa(z)\left(p'(z)\frac{\partial^2 D(p(z),\kappa(z))}{\partial p^2(z)} + \kappa'(z)\frac{\partial^2 D(p(z),\kappa(z))}{\partial \kappa(z)\partial p(z)}\right) \\ &+ C_1\left(\lambda\kappa(z)+\kappa'(z)\right) + \lambda C_2\kappa^2(z) = 0, \end{aligned} \quad (4.36)$$

We now consider the inequality in (4.24), where the l.h.s can be written as

$$\mathbb{E}_\pi\left[D^\dagger\left(p(Z),\frac{1}{\kappa^\epsilon(Z)}\right)\right] = \pi_0 D^\dagger\left(p(0),\kappa_0\right) + \int_{0^+}^L D^\dagger(p(z),\kappa^\epsilon(z))f(z)dz. \quad (4.37)$$

We compute $\kappa^\epsilon(z)$ using (4.11) as follows

$$\kappa^\epsilon(z) = \frac{1}{\frac{1}{\kappa(z)}+\epsilon g(z)}, \quad (4.38)$$

where its derivative with respect to ϵ at $\epsilon = 0$ can easily be obtained as below

$$\frac{d\kappa^{\epsilon}(z)}{d\epsilon}\Big|_{\epsilon=0} = -g(z)\kappa^2(z). \tag{4.39}$$

Similar to (4.29), we write the Taylor series of $D(p(z), \kappa^{\epsilon}(z))$ up to first order term in ϵ as below

$$D(p(z), \kappa^{\epsilon}(z)) = D(p(z), \kappa(z)) + \epsilon \frac{\partial D(p(z), \kappa(z))}{\partial \kappa(z)} \frac{d\kappa^{\epsilon}(z)}{d\epsilon}\Big|_{\epsilon=0} + O(\epsilon^2). \tag{4.40}$$

Therefore, by substituting (4.11), (4.39) and (4.40) into (4.37), this is then reduced to

$$\begin{aligned}
&\mathbb{E}_{\pi}\left[D^{\dagger}\left(p(Z), \frac{1}{\kappa^{\epsilon}(Z)}\right)\right] \\
&= \mathbb{E}_{\pi}\left[D^{\dagger}\left(p(Z), \frac{1}{\kappa(Z)}\right)\right] \\
&\quad + \epsilon \int_{0^+}^{L} \left(D(p(z), \kappa(z))g(z)f(z) - \frac{\partial D(p(z), \kappa(z))}{\partial \kappa(z)}\kappa(z)g(z)f(z)\right) dz.
\end{aligned} \tag{4.41}$$

By substituting (4.41) into (4.24) and neglecting the higher order terms of ϵ, we establish the following necessary condition for a local and therefore a global optimal mismatch factor $\kappa(z)$,

$$\int_{0^+}^{L} g(z)f(z)\left[D(p(z), \kappa(z)) - \frac{\partial D(p(z), \kappa(z))}{\partial \kappa(z)}\kappa(z)\right] dz = 0. \tag{4.42}$$

Equation (4.42) holds for all perturbation functions $g(z)$ that satisfy (4.21). Therefore, we rewrite (4.42) as

$$\int_{0^+}^{L} g(z)f(z)\left[D(p(z), \kappa(z)) - \frac{\partial D(p(z), \kappa(z))}{\partial \kappa(z)}\kappa(z) + \beta\right] dz = 0, \tag{4.43}$$

where β is a constant. Based on the fundamental lemma of the calculus of variations, we thus derive the following equation

$$D(p(z),\kappa(z)) - \frac{\partial D(p(z),\kappa(z))}{\partial \kappa(z)}\kappa(z) + \beta = 0, \quad z > 0. \tag{4.44}$$

Solutions to the equations in (4.35) and (4.44) determine structure of a locally optimal power policy $p(z)$ as well as a locally optimal mismatch factor policy $\kappa(z)$.

4.2.3 A structural result on the distortion

In this part, we discuss an interesting consequence of (4.44) on the instantaneous distortion $D(p(z),\kappa(z)), z > 0$. Specifically, we find below in Lemma 2 that a locally optimal solution has the property that the power policy and the mismatch factor policy are adjusted in such a way that, provided the battery has charge and thus the transmission power $p(z) > 0$, $D(p(z),\kappa(z))$ is constant for $z > 0$. In other words, if the transmission power is decreased (or increased) due to a change in the battery charge, a locally optimal mismatch factor will always dynamically adjust so that the instantaneous distortion is maintained to a constant level. As elaborated in section 3, one can think of the transmission power $p(z)$ and the mismatch factor $\kappa(z)$ as limited communication resources that must maintain long-term averages. Intuitively, this shows that the transmitter is trading off one resource for another. More precisely, since the mismatch factor must satisfy (3.4) (i.e., the inverse mismatch factor averages to one), as the availability of one communication resource (say the transmission power) increases due to a large battery charge, the transmitter employs a large transmission power and saves on the other communication resource (i.e., the mismatch factor) by then using fewer channel uses per source symbol. Likewise, when the battery charge is low, the transmitter reduces its transmission power, but employs a large mismatch factor. Formally,

we have the following Lemma.

Lemma 2. *The constant β in (4.44) must be in the range $\beta_{\min} < \beta < \beta_{\max}$ where*

$$\beta_{\max} = \lim_{D \downarrow 0} \quad \frac{R_s(D)}{R_s'(D)}, \tag{4.45}$$

and

$$\beta_{\min} = \lim_{D \uparrow D_{\max}} \quad \frac{R_s(D)}{R_s'(D)} - D_{\max}. \tag{4.46}$$

Furthermore, for every such a choice of β, (4.44) results in a unique constant solution for $D(p(z), \kappa(z)),\ z > 0$.

Proof. See Appendix A.2. □

Hence, for every fixed value of β the instantaneous distortion $D(p(z), \kappa(z))$ in (4.44) is independent of the power level $p(z)$ and the mismatch factor $\kappa(z)$ for $z > 0$. It is easy to verify that for both Gaussian and binary sources, $\lim_{D \downarrow 0} \quad \frac{R_s(D)}{R_s'(D)} = 0$ and $\lim_{D \uparrow D_{\max}} \quad \frac{R_s(D)}{R_s'(D)} = 0$. Therefore, for the Gaussian source we have the bound $-\sigma^2 < \beta < 0$. Likewise, for the binary source we have the bound $-\min\{\mathsf{p}, 1-\mathsf{p}\} < \beta < 0$.

4.3 A Constant Bandwidth Mismatch Factor

So far, we have studied a general JSCC scheme where the mismatch factor is adaptively adjusted according to the available battery charge. However it is also interesting to compare the results with the lower complexity case where the mismatch factor is fixed. Thus, we now consider the case where the mismatch factor is constant and does not adapt to the battery charge. For a fair comparison with the general case of dynamic mismatch factor, the constraint in (3.13) must still be satisfied which results in a constant bandwidth mismatch

factor of unity, i.e., $\kappa(z) = 1,\ \forall z \geq 0$. Therefore, there is only one design parameter, the transmission power $p(z)$, to be adapted to the battery charge to minimize the total average distortion at the receiver. We thus have

$$R_s(D(z)) = R_c\left(p\left(z\right)\right),$$

and thereby the distortion-rate function is computed only in terms of the transmission power $p(z)$. The optimization problem is therefore described as follows

$$\inf_{f(z),\pi_0} \quad \pi_0\tilde{D}(p(0)) + \int_{0^+}^{L} \tilde{D}\left(p(z)\right) f(z)dz \tag{4.47}$$

$$\text{subject to: } f(z)\left(p(z) + \ell(z)\right) = \delta e^{-\lambda z}\Big(\pi_0 + \int_{0^+}^{L} e^{\lambda u} f(u)du\Big) \tag{4.48}$$

$$\pi_0 + \int_{0^+}^{L} f(z)dz = 1 \tag{4.49}$$

$$f(z) \geq 0, \quad \pi_0 \geq 0, \tag{4.50}$$

where $\tilde{D}(p(z)) = D(p(z), 1)$ is the average distortion with bandwidth mismatch factor of unity. Moreover, the distortion lower bound in this case is the same as D_{LB} in (4.1).

4.3.1 Achievable Power Allocation

As a necessary condition for a local and thus a global optimal power policy $p(z)$, we can directly obtain the following equation by replacing $\kappa(z) = 1$ into (4.35) with the substitution $\lambda(C_1 + C_2) = C$,

$$\delta \int_{z}^{L} \tilde{D}'(p(u))e^{-\lambda(u-z)}du + \tilde{D}(p(z)) - \tilde{D}'(p(z))p(z) + C = 0, \tag{4.51}$$

where $\tilde{D}'(\cdot)$ denotes the derivative of $\tilde{D}(\cdot)$. As explained below (4.35), we can derive a first order non-linear autonomous ODE equivalent to (4.51). This yields

$$\lambda\tilde{D}(p(z)) + (\delta - \lambda p(z))\,\tilde{D}'(p(z)) + p(z)p'(z)\tilde{D}''(p(z)) + C = 0, \tag{4.52}$$

where $\tilde{D}''(\cdot)$ denotes the second derivative of $\tilde{D}(\cdot)$. The following lemma states an important property of solutions to (4.51).

Lemma 3. *Any solution $p(z)$ of (4.52) for $C < -\lambda\tilde{D}(\frac{\delta}{\lambda})$ is non-decreasing in z, for $p(z) > 0$.*

Proof. See Appendix A.3. □

Remark 3. *The constant C in (4.52) can be used as a degree of freedom to control the initial slope of the power policy $p'(0^+)$ (see Appendix A.3).*

4.4 Gaussian Source and Channel

In this section, we specialize our results for a Gaussian source using the rate-distortion function $R_s(D)$ given in (2.3). We assume that the Shannon rate function $R_c(p) = \frac{1}{2}\log_2(1+p/N)$ is considered for the channel coding rate. Consequently, the distortion function $D(p,\kappa)$ can be computed as

$$D(p(z),\kappa(z)) = \sigma^2\left(1+\frac{p(z)}{N}\right)^{-\kappa(z)}, \tag{4.53}$$

or equivalently

$$D^\dagger(p(z),1/\kappa(z)) = \frac{\sigma^2}{\kappa(z)}\left(1+\frac{p(z)}{N}\right)^{-\kappa(z)}. \tag{4.54}$$

Moreover, the lower bound on the average distortion in this case is

$$\mathbb{E}_\pi\left[D^\dagger\left(p(Z),\frac{1}{\kappa(Z)}\right)\right]\geq\sigma^2\left(1+\frac{\delta}{\lambda}\frac{\left(1-e^{-\lambda L}\right)}{N}\right)^{-1}. \tag{4.55}$$

To determine structure of an optimal achievable scheme, we first replace $D(p(z),\kappa(z))$ in (4.44) by its closed form expression in (4.53) to obtain

$$\sigma^2\left(1+\frac{p(z)}{N}\right)^{-\kappa(z)}\left(1+\kappa(z)\ln(1+\frac{p(z)}{N})\right)+\beta=0,\quad z>0, \tag{4.56}$$

which can be rewritten as

$$\left(-1-\kappa(z)\ln\left(1+\frac{p(z)}{N}\right)\right)\exp\left(-1-\kappa(z)\ln\left(1+\frac{p(z)}{N}\right)\right)=\frac{\beta}{\sigma^2 e}, \tag{4.57}$$

for $z>0$. Therefore, we have

$$\kappa\left(z;\beta\right)=-\frac{W_n\left(\frac{\beta}{\sigma^2 e}\right)+1}{\ln\left(1+\frac{p(z)}{N}\right)},\quad z>0, \tag{4.58}$$

where $W_n(\cdot)$ denotes the *LambertW* function [39] that takes either real or complex values and has an infinite number of branches, each denoted by an integer n. The notation $\kappa\left(z;\beta\right)$ emphasizes the dependence of $\kappa(z)$ in (4.58) depends on the choice of β. Moreover, (4.58) shows that $\kappa(z;\beta)$ is a decreasing function of z, whenever $p(z)$ is an increasing function of z and vice versa.

Proposition 1. *The only branch that results in positive values of* $\kappa(z;\beta)$ *in* (4.58)*, is* $n=-1$.

Proof. See Appendix A.4. □

From (4.58), for every fixed value of β, we have

$$-\frac{1}{2}\left(W_{-1}\left(\frac{\beta}{\sigma^2 e}\right)+1\right)\log_2 e = \kappa\left(z;\beta\right)\times\frac{1}{2}\log_2\left(1+\frac{p(z)}{N}\right),\quad z>0. \tag{4.59}$$

On the other hand, this choice of β results in the instantaneous distortion $D(z) := D(p(z),\kappa(z))$ in (2.7) as follows

$$\frac{1}{2}\log_2\frac{\sigma^2}{D(z)} = \kappa(z;\beta)\times\frac{1}{2}\log_2\left(1+\frac{p(z)}{N}\right),\quad z\geq 0. \tag{4.60}$$

Therefore, combining (4.59) and (4.60), we obtain

$$\ln\frac{\sigma^2}{D(z)} = -\left(W_{-1}\left(\frac{\beta}{\sigma^2 e}\right)+1\right),\quad z>0. \tag{4.61}$$

Eq. (4.61) also holds for the optimal choice of β (say $\beta^\star$) and the associated optimal instantaneous distortion $D^\star(z)$, for $z>0$. We thus compute the distortion $D^\star(z)$ in terms of $\beta^\star$, using (4.61), as

$$D^\star(z) = \begin{cases} \sigma^2\exp\left(W_{-1}\left(\dfrac{\beta^\star}{\sigma^2 e}\right)+1\right), & z>0,\\ \sigma^2, & z=0. \end{cases} \tag{4.62}$$

As elaborated in Appendix A.2, (4.62) is the unique constant solution of (4.44) for $z>0$ in the Gaussian case. Specifically, $p(z)$ and $\kappa(z)$ are jointly optimized such that when using a high (respectively low) transmission power, the transmitter uses a low (respectively high) mismatch factor to maintain the optimal instantaneous distortion to a constant value.

Chapter 5

Numerical Results

In this section, we consider numerical solutions to (4.35) and (4.44) to obtain an efficient power policy $p(z)$ and mismatch factor policy $\kappa(z)$. In particular, although there is no apparent closed-form solution to (4.35) for $p(z)$, for every choice of the constants C_1, C_2 and the initial condition $p(0^+)$, we can apply numerical ODE solution methods. More precisely, given a fixed choice of β, from (4.44) we can in principle solve for $\kappa(z)$ in terms of $p(z)$ (although other than the Gaussian case where a closed-form is found in (4.58), this must be done numerically). We then substitute $\kappa(z)$ thus computed into (4.35) and obtain an ODE for $p(z)$ in terms of C_1, C_2 and β that can be solved numerically. Once $p(z)$ is thus found, one can then directly obtain $\kappa(z)$ using (4.44) again.

We obtain from (2.20) that

$$\frac{f(z)e^{\lambda z}}{\pi_0 + \int_{0^+}^{z} e^{\lambda u} f(u)du} = \frac{\delta}{p(z) + \ell(z)}, \tag{5.1}$$

where by integrating both sides over $(0^+, z]$ and performing some simplifications, this is

recast as

$$\pi_0 + \int_{0^+}^{z} e^{\lambda u} f(u) du = \pi_0 \exp\left(\int_{0^+}^{z} \frac{\delta}{p(u) + \ell(u)} du \right). \tag{5.2}$$

Taking the derivative of both sides in (5.2) with respect to z, we compute the density $f(z)$, provided that π_0 is known, as follows

$$f(z) = \pi_0 \frac{\delta e^{-\lambda z}}{p(z) + \ell(z)} \exp\left(\int_{0^+}^{z} \frac{\delta}{p(u) + \ell(u)} du \right). \tag{5.3}$$

By combining (5.3) and (3.12), we compute the atom π_0 as below

$$\pi_0 = \left(1 + \int_{0^+}^{L} \frac{\delta e^{-\lambda z}}{p(z) + \ell(z)} \exp\left(\int_{0^+}^{z} \frac{\delta}{p(u) + \ell(u)} du \right) dz \right)^{-1}. \tag{5.4}$$

Moreover, the value of the mismatch factor $\kappa_0 := \kappa(z)|_{z=0}$ when the battery is dead is obtained from (3.13) as

$$\kappa_0 = \frac{\pi_0}{1 - \int_{0^+}^{L} f(z)/\kappa(z;\beta) dz}. \tag{5.5}$$

We now study a single-user EH communication system with energy arrival rates $\delta = \lambda = 1$, and noise power $N = 1$. To find locally optimal policies for $p(z)$ and $\kappa(z)$, one needs to search for the optimized values of the free constants β, C_1, and C_2. In the following we separately investigate the cases of Gaussian and binary sources.

5.0.1 A Gaussian Source over a Gaussian Channel

For a standard Gaussian source $\mathcal{N}(0,1)$, we have the bound $-1 < \beta < 0$ from subsection 4.2.3. We now examine two cases of leakage: (i) zero leakage rate $\ell(z) = 0$ for an ideal battery and (ii) non-zero leakage rate $\ell(z) = 1 - e^{-z}$ for an imperfect battery. We also consider the battery capacities $L = 1, 2, ..., 5$. Table 5.1 and Table 5.2 show the total average

Table 5.1: Distortion lower bound (D_{LB}), average distortion (D_{avg}), and good values of the constants C_1, C_2 and β of a standard Gaussian source $\mathcal{N}(0,1)$, for different battery capacities with the initial condition $p(0^+) = 0.001$, when $\ell(z) = 0$. The ratio of D_{avg} to D_{LB} quantifies the gap between the average distortion and the lower bound.

Capacity of the Battery	D_{LB}	D_{avg}	$D_{\mathrm{avg}}/D_{\mathrm{LB}}$	Constants
$L = 1$	0.6127	0.6992	1.14	$\beta = -0.9493, C_1 = -1.00, C_2 = 0.20$
$L = 2$	0.5363	0.6110	1.13	$\beta = -0.9156, C_1 = -1.00, C_2 = 0.30$
$L = 3$	0.5128	0.5780	1.12	$\beta = -0.8947, C_1 = -0.90, C_2 = 0.30$
$L = 4$	0.5046	0.5571	1.10	$\beta = -0.8829, C_1 = -0.90, C_2 = 0.32$
$L = 5$	0.5017	0.5431	1.08	$\beta = -0.8745, C_1 = -0.90, C_2 = 0.34$

Table 5.2: Distortion lower bound (D_{LB}), average distortion (D_{avg}), and good values of the constants C_1, C_2 and β of a standard Gaussian source $\mathcal{N}(0,1)$, for different battery capacities with the initial condition $p(0^+) = 0.001$, when $\ell(z) = 1 - e^{-z}$. The ratio of D_{avg} to D_{LB} quantifies the gap between the average distortion and the lower bound.

Capacity of the Battery	D_{LB}	D_{avg}	$D_{\mathrm{avg}}/D_{\mathrm{LB}}$	Constants
$L = 1$	0.6127	0.7706	1.25	$\beta = -0.9000, C_1 = -0.90, C_2 = 0.08$
$L = 2$	0.5363	0.7078	1.31	$\beta = -0.9000, C_1 = -0.90, C_2 = 0.17$
$L = 3$	0.5128	0.6838	1.33	$\beta = -0.9000, C_1 = -0.90, C_2 = 0.26$
$L = 4$	0.5046	0.6760	1.34	$\beta = -0.9000, C_1 = -0.90, C_2 = 0.29$
$L = 5$	0.5017	0.6726	1.34	$\beta = -0.8997, C_1 = -0.90, C_2 = 0.30$

distortion D_{avg}, the distortion lower bound D_{LB}, and good values of the constants β, C_1, and C_2 found by numerical search for both cases. Furthermore, the initial condition of the ODE for $p(z)$ was chosen to be $p(0^+) = 0.001$. This choice of $p(0^+)$ is justified by the fact that a small amount of available energy in the battery should entail a small transmission power, as otherwise, the battery will be completely depleted before the next energy arrival. It is evident from Table 5.1 that as the battery capacity increases, the gap between the achieved distortion and the lower bound diminishes. In particular, for $L = 5$ when the leakage rate is zero this scheme can achieve a distortion which is at most 8% above the lower bound. In fact, for an ideal battery with infinite capacity as discussed below (4.5) the lower bound is asymptotically tight and can be achieved via a constant transmission power policy and a

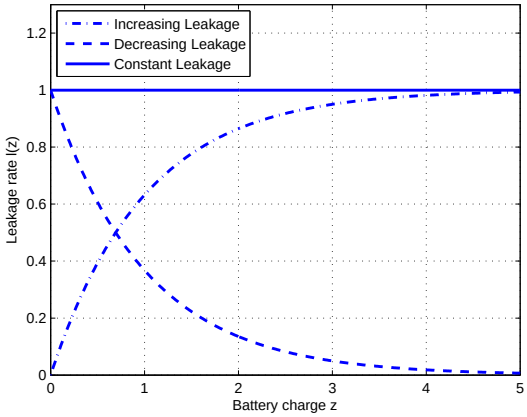

Figure 5.1: Different functions for the leakage rate $\ell(z)$, i.e., increasing $\ell(z) = 1 - e^{-z}$, decreasing $\ell(z) = e^{-z}$, and constant $\ell(z) = 1$.

constant mismatch factor policy. Moreover, for case (ii) with non-zero leakage, the achieved average distortions are larger compared to that of case (i). Since the lower bound in Table 5.2 is potentially looser now, the gap between the achieved average distortion and the lower bound in this case does not necessarily follow the same trend as in the Table 5.1.

Fig. 5.2 shows the transmission power policy $p(z)$, for to the case of $L = 5$, for an ideal battery as well as an imperfect battery with three different leakage rates $\ell(z)$ (i.e., increasing, decreasing and constant) as shown in Fig. 5.1. We observe that in all cases, the designed transmission power monotonically increases as the battery charge increases. This is due to the fact that when the remaining charge in the battery is close to the capacity limit, new energy arrivals are likely to overflow the battery. Therefore, the transmitter consumes a large transmission power in order to avoid lost energy. Interestingly, for the increasing leakage and the constant leakage cases, the allocated transmission power increases faster with battery charge level compared to the transmission power for an ideal battery. This result is intuitive, since an efficient transmission power policy mitigates the large energy loss due to leakage by rapidly consuming the stored energy before it is lost. Fig. 5.3 and

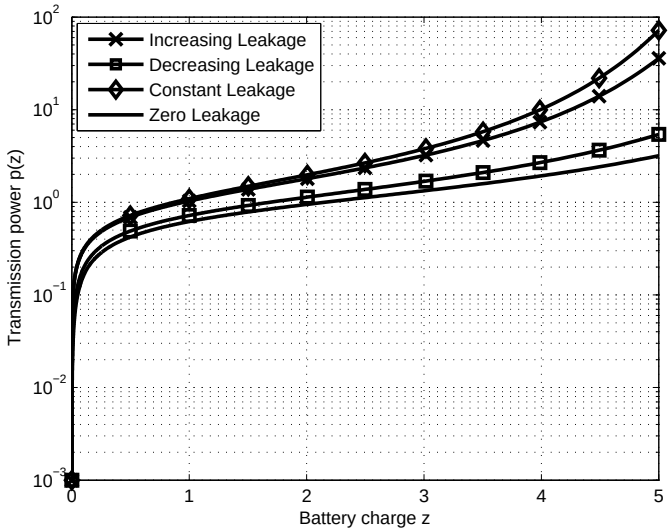

Figure 5.2: Power policy $p(z)$ under 4 different scenarios, namely, zero leakage, constant non-zero leakage, i.e., increasing and decreasing leakage, when $p(0^+) = 0.001$.

5.4 illustrate the corresponding mismatch factor $\kappa(z)$ and absolutely continuous part of the density function of the available charge in the battery, respectively. It can be seen that as the energy in the battery decreases, the mismatch factor increases. In other words, the low transmission power due to reduced charge in the battery is compensated by using longer channel codewords. Conversely, when the transmission power is large, smaller codewords are used so that the constraint in (3.4) is satisfied. As expected, an increasing transmission power results in a decreasing density function $f(z)$. In other words, the storage process spends a smaller fraction of time at higher battery charges that have larger transmission power.

The average distortion for the two cases of dynamically varying bandwidth mismatch factor and constant bandwidth mismatch factor is illustrated in Fig 5.5, both as functions of battery capacity. It can be observed that for a battery with capacity in the range $2 \leq L \leq 7$, a communication system with an adaptive mismatch factor, as proposed in this paper, performs

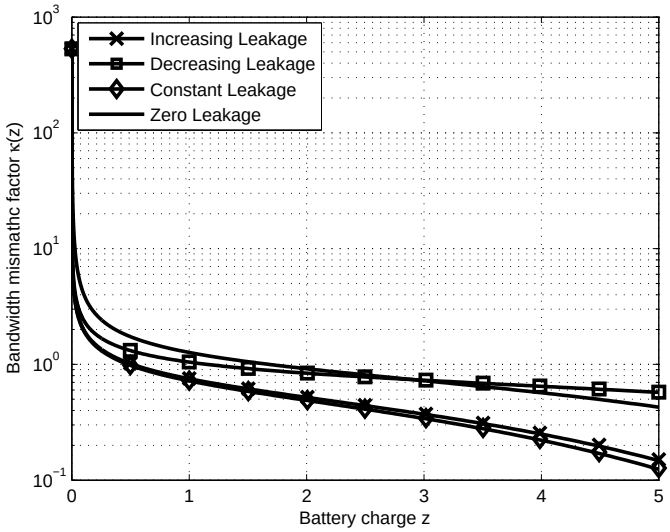

Figure 5.3: Bandwidth mismatch factor $\kappa(z)$ under 4 different scenarios, namely, zero leakage, constant non-zero leakage, i.e., increasing and decreasing leakage, when $p(0^+) = 0.001$.

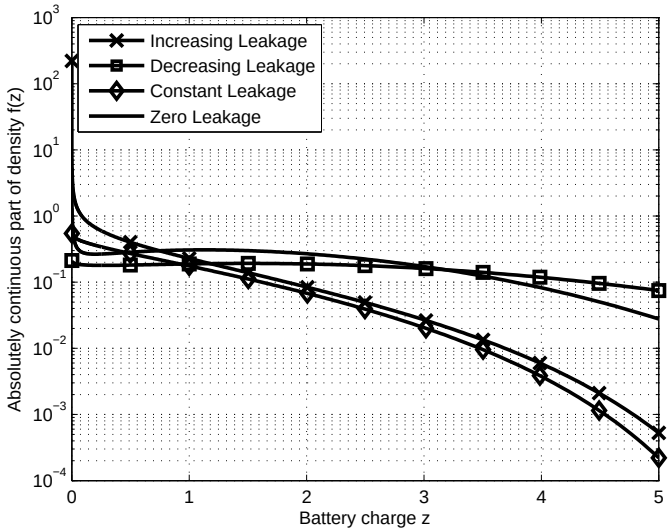

Figure 5.4: Density function $f(z)$ under 4 different scenarios, namely, zero leakage, constant non-zero leakage, i.e., increasing and decreasing leakage, when $p(0^+) = 0.001$.

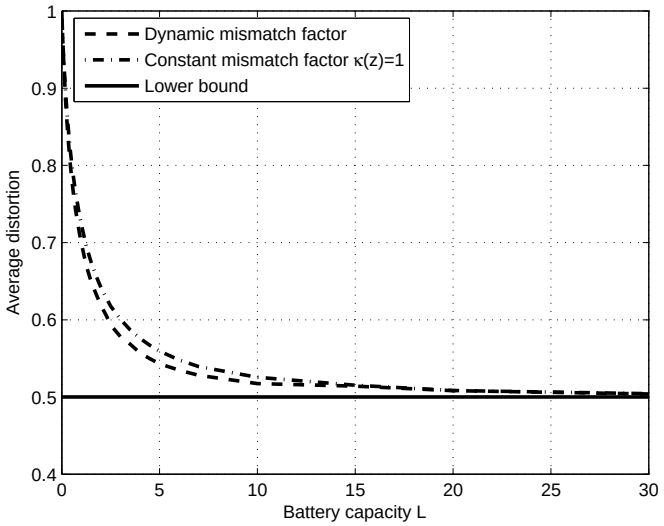

Figure 5.5: Average distortion for the two cases of adaptive mismatch factor and constant mismatch factor $\kappa(z) = 1$, when the battery capacity varies in the range $0 \leq L \leq 30$.

better compared to that of $\kappa(z) = 1$. On the other hand, regardless of whether or not we are using a dynamic mismatch factor or a constant mismatch factor, for large battery capacities the average distortion of both coding schemes approach the lower bound and merge eventually. Likewise, for small battery capacities the average distortion of both coding schemes approach $D_{\max}$ and merge as well.

5.0.2 A Binary Source over a Gaussian Channel

We now consider a binary source with the Bernoulli(1/2) distribution for which we have $H(\mathsf{p}) = 1$, and the bound $-0.5 < \beta < 0$ as explained in subsection 4.2.3. Analogous to the Gaussian source, with different battery capacities $L = 1, 2, ..., 5$ and for the two cases of (i) zero leakage rate $\ell(z) = 0$ and (ii) non-zero leakage rate $\ell(z) = 1 - e^{-z}$, we evaluate the achieved average distortion D_{avg}, the distortion lower bound D_{LB} and good values of

Table 5.3: Distortion lower bound (D_{LB}), average distortion (D_{avg}), and good values of the constants C_1, C_2 and β of a Bernoulli(1/2) source, for different battery capacities with the initial condition $p(0^+) = 0.001$, when $\ell(z) = 0$. The ratio of D_{avg} to D_{LB} quantifies the gap between the average distortion and the lower bound.

Capacity of the Battery	D_{LB}	D_{avg}	$D_{\mathrm{avg}}/D_{\mathrm{LB}}$	Constants
$L = 1$	0.1651	0.2195	1.32	$\beta = -0.3448, C_1 = -0.35, C_2 = 0.10$
$L = 2$	0.1270	0.1669	1.31	$\beta = -0.3178, C_1 = -0.35, C_2 = 0.15$
$L = 3$	0.1161	0.1494	1.28	$\beta = -0.3054, C_1 = -0.35, C_2 = 0.16$
$L = 4$	0.1122	0.1400	1.24	$\beta = -0.2985, C_1 = -0.35, C_2 = 0.19$
$L = 5$	0.1108	0.1331	1.20	$\beta = -0.2939, C_1 = -0.35, C_2 = 0.19$

Table 5.4: Distortion lower bound (D_{LB}), average distortion (D_{avg}), and good values of the constants C_1, C_2 and β of a Bernoulli(1/2) source, for different battery capacities with the initial condition $p(0^+) = 0.001$, when $\ell(z) = 1 - e^{-z}$. The ratio of D_{avg} to D_{LB} quantifies the gap between the average distortion and the lower bound.

Capacity of the Battery	D_{LB}	D_{avg}	$D_{\mathrm{avg}}/D_{\mathrm{LB}}$	Constants
$L = 1$	0.1651	0.2732	1.65	$\beta = -0.3000, C_1 = -0.30, C_2 = 0.10$
$L = 2$	0.1270	0.1943	1.52	$\beta = -0.3000, C_1 = -0.30, C_2 = 0.14$
$L = 3$	0.1161	0.1540	1.32	$\beta = -0.3000, C_1 = -0.30, C_2 = 0.15$
$L = 4$	0.1122	0.1447	1.28	$\beta = -0.3000, C_1 = -0.30, C_2 = 0.18$
$L = 5$	0.1108	0.1358	1.22	$\beta = -0.2950, C_1 = -0.30, C_2 = 0.18$

the constants found by numerical search. The results of case (i) and (ii) are summarized in Table 5.3 and Table 5.4, respectively. Similar to the Gaussian case, we observe that as the battery capacity increases the relative gap between the achieved average distortion and the lower bound diminishes. Particularly, the numerical results further show that for $L = 5$ the proposed achievable scheme with no leakage can achieve a distortion which is at most 20% above the lower bound.

Chapter 6

Conclusion and Future Work

6.1 Conclusion

We have investigated the problem of joint source-channel coding in a point-to-point channel with an energy harvesting transmitter.

We used a calculus of variations technique to characterize an achievable joint source-channel coding scheme as well as an achievable transmission power policy to minimize the distortion at the receiver. We also obtained a distortion lower bound, where we used the convexity of the distortion function and an upper bound on the average transmission power.

For a moderate-size battery capacity, we numerically showed that the achievable distortion with a dynamically varying bandwidth mismatch factor is smaller than that of a constant mismatch factor. However, when the battery capacity is large or small, the distortion performance does not significantly improve with an adaptive mismatch factor compared to a constant mismatch factor. Moreover, we observed that as the battery capacity tends to infinity the achievable distortion for both coding schemes approached the lower bound.

Furthermore, with a constant mismatch factor $\kappa(z) = 1$, we found a constant transmission power policy that can achieve this lower bound for an infinite battery capacity.

As examples of continuous and discrete alphabet sources, we considered both Gaussian and binary sources to validate our analytical findings. In both cases, we showed numerically that a good transmission power policy increases as the battery charge increases. In contrast, the mismatch factor which measures the ratio of the length of channel codewords per source symbol, is a decreasing function of the battery charge. We further examined these policies under different possibilities for battery leakage rate, i.e., zero leakage rate as well as non-zero arbitrary leakage rate.

6.2 Future Work

In real applications, the delay by which the source symbols are reconstructed at the receiver plays an important role in the performance analysis of lossy communication systems that has to be taken into account. Therefore, an interesting future extension of this work could be a finite-time horizon counterpart of this problem setting under a delay constraint for the reconstruction of symbols. In such a case, the problem can be solved numerically using dynamic-programming approaches and Bellman's equation.

Another interesting extension, is to consider a data buffer with finite capacity whose knowledge could be known at the transmitter either casually or non-causally. Then, the communication resources must be adaptively allocated according to the current state of the data buffer as well as available battery charge.

As discussed in Chapter 3, the lower bound on the total average distortion is loose in the general case of finite battery capacity. Therefore, another line of future directions could be

reducing the gap between the achievable scheme and the lower bound by either establishing a tighter bound or improving the achievable scheme.

As discussed in Chapter 2, we only considered a Poisson energy arrival process for which an elegant dam storage model can be applied to identify an ergodic battery charge process. Other energy arrival processes could be considered to model the EH process, as another line of work.

Finally, we have studied the design of optimal communication resources (i.e., transmission power and mismatch factor) in EH communication systems to minimize the total average distortion at the receiver. Another interesting future work could be designing optimal MAC and routing protocols in an EH sensor network.

Appendix A

APPENDICES

A.1 Proof of Convexity

To prove the convexity of the distortion function $D^\dagger(p,q)$ over the domain $p \geq 0, q > 0$ where $q := 1/\kappa$, we consider two cases: (a) $R_s^{\text{th}} = \infty$, (b) $R_s^{\text{th}} < \infty$. As already discussed, an example of the first case is a Gaussian source and an example of the second case is a binary source. We first prove the joint convexity with respect to p and q for case (a). To do so, we compute the Hessian matrix of $D^\dagger(p,q)$ for $p > 0, q > 0$, denoted by H, and show that it is positive definite. The Hessian is given by

$$H = \begin{pmatrix} \dfrac{\partial^2 D^\dagger}{\partial p^2} & \dfrac{\partial^2 D^\dagger}{\partial p\, \partial q} \\ \dfrac{\partial^2 D^\dagger}{\partial q\, \partial p} & \dfrac{\partial^2 D^\dagger}{\partial q^2} \end{pmatrix},$$

where by a simple calculation we obtain

$$H_{11} := \frac{\partial^2 D^\dagger}{\partial p^2}$$

$$= \frac{R_c''(p)}{R_s'\left(D(p,\kappa)\right)} + \left(R_c'(p)\right)^2 \kappa \times \frac{-R_s''\left(D(p,\kappa)\right)}{\left(R_s'(D(p,\kappa))\right)^3}$$
$$\overset{(a)}{>} 0,$$

where (a) follows from the conditions $[S2]$ and $[C2]$ on $R_s(D)$ and $R_c(p)$, respectively. Moreover, the strict inequality is justified by the fact that since $R_s^{\text{th}} = \infty$, the distortion D is strictly positive and therefore $R_s'(D)$ is finite due to $[S3]$. Similarly, we can show that the determinant of H is strictly positive, i.e.,

$$\det(H) = \left(R_c(p)\right)^2 \kappa^3 R_c''(p) \times \frac{1}{R_s'(D(p,\kappa))} \times \frac{-R_s''(D(p,\kappa))}{R_s'(D(p,\kappa))}$$
$$\overset{(b)}{>} 0,$$

where (b) again follows from conditions $[S2]$, $[C2]$ and $[S3]$. Since, $H_{11} > 0$ and $\det(H) > 0$, by Sylvester's criterion the matrix H is positive definite, and it thus follows that $D^\dagger(p,q)$ is jointly convex over the pair p and q.

To prove the joint convexity with respect to p and q for case (b) where $R_s^{\text{th}} < \infty$, one should recall that $D^\dagger(p,q) = 0$ for $R_c(p) \geq qR_s^{\text{th}}$. Although the function $D^\dagger(p,q)$ is continuous everywhere, and in particular at the points where $\kappa R_c(p) = R_s^{\text{th}}$, the second derivative at these points may not necessarily exist and a more complicated analysis is required. Therefore, as illustrated in Fig. A.1 we separate the region $p > 0$ and $q > 0$ into two parts: the open shaded region, $R_c(p) < qR_s^{\text{th}}$, over which the convexity argument reduces to the case (a) and the closed white region, $R_c(p) \geq qR_s^{\text{th}}$, over which $D^\dagger(p,q) = 0$. It is not hard to see that the white region given by $R_c(p) \geq qR_s^{\text{th}}$ (or equivalently $q \leq R_c(p)/R_s^{\text{th}}$) is convex. This is due to the fact that $R_c(p)$ is a concave function and thus the region it traces is convex. Now, consider two arbitrary points $\alpha_1 = (p_1, q_1)$ and $\alpha_2 = (p_2, q_2)$ such that

$\alpha_1, \alpha_2 \in \{(p,q) : p > 0, q > 0\}$. For $\lambda \in [0,1]$, we first define the function $g(\lambda)$ as follows

$$\begin{aligned} g(\lambda) :=& \; D^\dagger\left(\lambda\alpha_1 + (1-\lambda)\alpha_2\right) \\ =& \; D^\dagger(\lambda p_1 + (1-\lambda)p_2, \lambda q_1 + (1-\lambda)q_2). \end{aligned}$$

If $g(\lambda)$ is convex for all choices of α_1 and α_2, then so is $D^\dagger(p,q)$. With respect to the closed line segment connecting these two points (i.e., $\mathcal{L} = \{\lambda\alpha_1 + (1-\lambda)\alpha_2 : \lambda \in [0,1]\}$), five different cases may happen. First, if α_1 and α_2 are both in the white region, the line segment $\mathcal{L}$ only passes through the white region as the region is convex and thus $g(\lambda) = 0$, which is convex. If α_1 and α_2 are both in the shaded region, then either $\mathcal{L}$ only passes through the shaded region where the convexity of $g(\lambda)$ reduces to the case (a), or due to the convexity of the white region it enters the white region for one and only one contiguous closed interval $[\lambda_2, \lambda_3] \subset (0,1)$ and again returns to the shaded region for $\lambda > \lambda_3$. The function $g(\lambda)$ in the latter case is continuous for $\lambda \in [0,1]$, non-negative and strictly convex for $\lambda \in [0,\lambda_2) \cup (\lambda_3, 1]$, while $g(\lambda) = 0$ for $\lambda \in [\lambda_2, \lambda_3]$. Thus, $g(\lambda)$ is convex and this case is illustrated in Fig. A.2b. If α_1 and α_2 are in two different regions (say α_1 is in the white region and α_2 is in the shaded region), there exists $\lambda_1 \in (0,1]$ as shown in Fig. A.2a such that $\mathcal{L}$ lies in the shaded region for $\lambda < \lambda_1$ and it enters the white region for $\lambda \geq \lambda_1$. Furthermore, once the line segment enters the convex white region, it does not exit. Here, $g(\lambda)$ is again continuous for $\lambda \in [0,1]$, non-negative and strictly convex for $\lambda \in [0,\lambda_1)$, while $g(\lambda) = 0$ for $\lambda \in [\lambda_1, 1]$. Thus, $g(\lambda)$ is convex. Similarly, when α_1 is in the shaded region and α_2 is in the white region we have Fig. A.2c, where $g(\lambda)$ is convex. Consequently, even for sources for which zero distortion can be achieved the function $D^\dagger(p,q)$ is jointly convex over the pair p and q. This completes the proof.

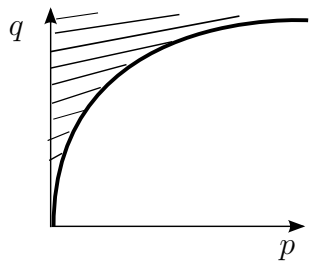

Figure A.1: The shaded region shows the area where $q > R_c(p)/R_s^{\text{th}}$.

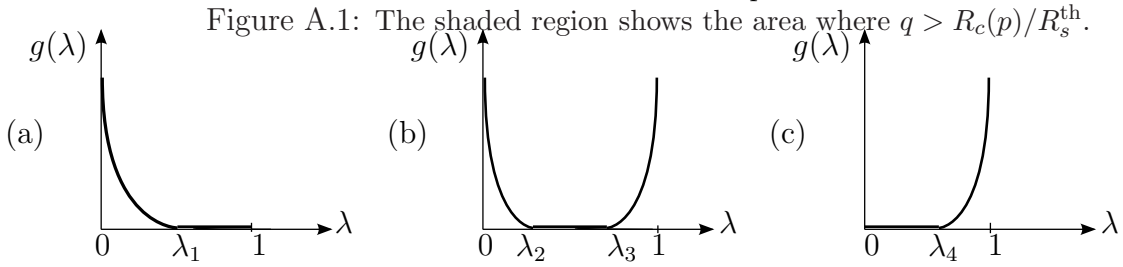

Figure A.2: Special cases of the function $g(\lambda)$.

A.2 Instantanous Distortion

We first rewrite (2.7) for $z > 0$ as

$$R_s(D(p(z), \kappa(z))) = \kappa(z) R_c(p(z)), \tag{A.1}$$

where by taking the first derivative of both sides with respect to $\kappa(z)$ at a fixed $z > 0$ we obtain

$$\frac{\partial D(p(z), \kappa(z))}{\partial \kappa(z)} R_s' \left(D \left(p(z), \kappa(z) \right) \right) = R_c(p(z)), \tag{A.2}$$

or equivalently

$$\frac{\partial D(p(z), \kappa(z))}{\partial \kappa(z)} = \frac{R_c(p(z))}{R_s' \left(D \left(p(z), \kappa(z) \right) \right)}. \tag{A.3}$$

With the substitution (A.3), (4.44) for $z > 0$ reduces to

$$D(p(z), \kappa(z)) - \frac{R_s(D(p(z), \kappa(z)))}{R_s' \left(D \left(p(z), \kappa(z) \right) \right)} + \beta = 0, \tag{A.4}$$

where for the second term we also used the substitution (A.1). Therefore, for each $z > 0$, $D(p(z), \kappa(z))$ must be a root of (A.4). To simplify notation, we fix $z > 0$, and simply write D in place of $D(p(z), \kappa(z))$. Solving (A.4) for β, we then obtain

$$\beta = \frac{R_s(D)}{R_s'(D)} - D. \tag{A.5}$$

We next show that the r.h.s of (A.5) is strictly decreasing with respect to D. To do so, we take the first derivative of the r.h.s in (A.5) with respect to D, and show that it is always negative in the open interval $0 < D < D_{\max}$, i.e.,

$$\frac{d}{dD}\left[\frac{R_s(D)}{R_s'(D)} - D\right] = \frac{\left(R_s'(D)\right)^2 - R_s''(D)R_s(D)}{\left(R_s'(D)\right)^2} - 1 \tag{A.6}$$

$$= \frac{-R_s''(D)R_s(D)}{\left(R_s'(D)\right)^2} \tag{A.7}$$

$$< 0, \tag{A.8}$$

where (A.8) follows from the assumption of $R_s''(D) > 0$ and further recalling that $R_s(D) > 0$ and $R_s'(D)$ is finite, for $0 < D < D_{\max}$. Therefore, for every fixed β, there is at most one real root D that solves (A.5), and it does not depend on z. This is also true for the optimized value of $\beta^\star$, and therefore the associated instantaneous distortion $D^\star(p(z), \kappa(z))$ is constant for $z > 0$. Furthermore, for there to be at least one real root, β in (A.5) must be in the range $\beta_{\min} < \beta < \beta_{\max}$, where

$$\beta_{\max} = \sup_{0<D<D_{\max}} \left[\frac{R_s(D)}{R_s'(D)} - D\right] \tag{A.9}$$

$$= \lim_{D \downarrow 0} \frac{R_s(D)}{R_s'(D)}, \tag{A.10}$$

and

$$\beta_{\min} = \inf_{0<D<D_{\max}} \left[\frac{R_s(D)}{R_s'(D)} - D \right] \tag{A.11}$$

$$= \lim_{D \uparrow D_{\max}} \frac{R_s(D)}{R_s'(D)} - D_{\max}. \tag{A.12}$$

A.3 Non-decreasing Power Policy

Solving (4.52) for $p'(z)$ we obtain

$$p'(z) = \frac{(\delta - \lambda p(z))\, \tilde{D}'(p(z)) + \lambda \tilde{D}(p(z)) + C}{-p(z)\tilde{D}''(p(z))}. \tag{A.13}$$

Now, it can be seen that the constant C is a degree of freedom that can be used to control the initial slope $p'(0^+)$ of the power policy.

Clearly, $\tilde{D}''(p(z)) > 0$, and from the first constraint on feasible power policies we have that $p(z) > 0$. Therefore, the denominator of (A.13) is negative for $z > 0$, and $p'(z) \geq 0$ if

$$C < -\left[(\delta - \lambda p(z))\, \tilde{D}'(p(z)) + \lambda \tilde{D}(p(z)) \right]. \tag{A.14}$$

We next find the global minimum for the r.h.s of (A.14). To do so, we must have

$$\frac{d}{dp(z)} \left[(\delta - \lambda p(z))\, \tilde{D}'(p(z)) + \lambda \tilde{D}(p(z)) \right] = (\delta - \lambda p(z))\, \tilde{D}''(p(z))$$

$$= 0. \tag{A.15}$$

We note that $\tilde{D}''(p(z)) \neq 0$, and therefore $p(z) = \delta/\lambda$ is where the global minimum of the r.h.s of (A.14) occurs. Substituting $p(z) = \delta/\lambda$ into (A.14), it is then reduced to the sufficient

condition $C < -\lambda\tilde{D}(\delta/\lambda)$ and the proof is complete.

A.4 LambertW Function

Based on the properties of the *LambertW* function [39], $n = 0$ and $n = -1$ are the only branches that yield a real value for $W_n(x)$, where $W_0(x) \geq -1$ for $x \geq -1/e$ and $W_{-1}(x) < -1$ for $-1/e < x < 0$. In addition, we require that $W_n(\frac{\beta}{\sigma^2 e}) < -1$ in (4.58) in order to have $\kappa(z;\beta) > 0$. Therefore, $n = -1$ is the only acceptable branch. This provides another proof for the fact that $-1/e < \frac{\beta}{\sigma^2 e} < 0$ or equivalently $-\sigma^2 < \beta < 0$.

References

[1] P. Corke, T. Wark, R. Jurdak, W. Hu, P. Valencia, and D. Moore, "Environmental wireless sensor networks," *Proceedings of the IEEE*, vol. 98, no. 11, pp. 1903–1917, 2010.

[2] R. Jafari, A. Encarnacao, A. Zahoory, F. Dabiri, H. Noshadi, and M. Sarrafzadeh, "Wireless sensor networks for health monitoring," in *Mobile and Ubiquitous Systems: Networking and Services, 2005. MobiQuitous 2005. The Second Annual International Conference on*, pp. 479–481, IEEE, 2005.

[3] D. Chen, Z. Liu, L. Wang, M. Dou, J. Chen, and H. Li, "Natural disaster monitoring with wireless sensor networks: a case study of data-intensive applications upon low-cost scalable systems," *Mobile Networks and Applications*, vol. 18, no. 5, pp. 651–663, 2013.

[4] C. Schurgers and M. B. Srivastava, "Energy efficient routing in wireless sensor networks," in *Military Communications Conference, 2001. MILCOM 2001. Communications for Network-Centric Operations: Creating the Information Force. IEEE*, vol. 1, pp. 357–361, IEEE, 2001.

[5] Y. Yu, R. Govindan, and D. Estrin, "Geographical and energy aware routing: A recursive data dissemination protocol for wireless sensor networks," tech. rep., Technical report ucla/csd-tr-01-0023, UCLA Computer Science Department, 2001.

[6] G. Li and R. Doss, "Energy-efficient medium access control in wireless sensor networks," in *Guide to wireless sensor networks*, pp. 419–438, Springer, 2009.

[7] V. Rajendran, K. Obraczka, and J. J. Garcia-Luna-Aceves, "Energy-efficient, collision-free medium access control for wireless sensor networks," *Wireless Networks*, vol. 12, no. 1, pp. 63–78, 2006.

[8] V. Raghunathan, A. Kansal, J. Hsu, J. Friedman, and M. Srivastava, "Design considerations for solar energy harvesting wireless embedded systems," in *Proceedings of the 4th international symposium on Information processing in sensor networks*, p. 64, IEEE Press, 2005.

[9] Y. K. Tan and S. K. Panda, "Optimized wind energy harvesting system using resistance emulator and active rectifier for wireless sensor nodes," *Power Electronics, IEEE Transactions on*, vol. 26, no. 1, pp. 38–50, 2011.

[10] V. Leonov, T. Torfs, P. Fiorini, and C. Van Hoof, "Thermoelectric converters of human warmth for self-powered wireless sensor nodes," *Sensors Journal, IEEE*, vol. 7, no. 5, pp. 650–657, 2007.

[11] M. Gastpar, "Uncoded transmission is exactly optimal for a simple gaussian sensor network," *Information Theory, IEEE Transactions on*, vol. 54, no. 11, pp. 5247–5251, 2008.

[12] U. Mittal and N. Phamdo, "Hybrid digital-analog (hda) joint source-channel codes for broadcasting and robust communications," *Information Theory, IEEE Transactions on*, vol. 48, no. 5, pp. 1082–1102, 2002.

[13] Z. Reznic, M. Feder, and R. Zamir, "Distortion bounds for broadcasting with bandwidth expansion," *Information Theory, IEEE Transactions on*, vol. 52, no. 8, pp. 3778–3788, 2006.

[14] M. P. Wilson, K. Narayanan, and G. Caire, "Joint source channel coding with side information using hybrid digital analog codes," *Information Theory, IEEE Transactions on*, vol. 56, no. 10, pp. 4922–4940, 2010.

[15] C. Tian and S. Shamai, "Sending gaussian source on bandwidth-mismatched gaussian channel with improved robustness," in *Communications (ICC), 2011 IEEE International Conference on*, pp. 1–5, IEEE, 2011.

[16] Y. Zhao, B. Chen, and R. Zhang, "Optimal power allocation for an energy harvesting estimation system," in *Acoustics, Speech and Signal Processing (ICASSP), 2013 IEEE International Conference on*, pp. 4549–4553, IEEE, 2013.

[17] P. Castiglione, O. Simeone, E. Erkip, and T. Zemen, "Energy management policies for energy-neutral source-channel coding," *Communications, IEEE Transactions on*, vol. 60, no. 9, pp. 2668–2678, 2012.

[18] P. Castiglione and G. Matz, "Energy-neutral source-channel coding with battery and memory size constraints,"

[19] C. Tapparello, O. Simeone, and M. Rossi, "Dynamic compression-transmission for energy-harvesting multihop networks with correlated sources," 2012.

[20] O. Orhan, D. Gunduz, and E. Erkip, "Delay-constrained distortion minimization for energy harvesting transmission over a fading channel," in *Information Theory Proceedings (ISIT), 2013 IEEE International Symposium on*, pp. 1794–1798, IEEE, 2013.

[21] A. Limmanee, S. Dey, and A. Ahlén, "Distortion minimization via multiple sensors under energy harvesting constraints," in *Signal Processing Advances in Wireless Communications (SPAWC), 2013 IEEE 14th Workshop on*, pp. 225–229, IEEE, 2013.

[22] A. Nayyar, T. Basar, D. Teneketzis, and V. V. Veeravalli, "Optimal strategies for communication and remote estimation with an energy harvesting sensor," *Automatic Control, IEEE Transactions on*, vol. 58, no. 9, pp. 2246–2260, 2013.

[23] J. Yang and S. Ulukus, "Optimal packet scheduling in a multiple access channel with energy harvesting transmitters," *Communications and Networks, Journal of*, vol. 14, no. 2, pp. 140–150, 2012.

[24] K. Tutuncuoglu and A. Yener, "Optimum transmission policies for battery limited energy harvesting nodes," *Wireless Communications, IEEE Transactions on*, vol. 11, no. 3, pp. 1180–1189, 2012.

[25] J. Yang, O. Ozel, and S. Ulukus, "Broadcasting with an energy harvesting rechargeable transmitter," *Wireless Communications, IEEE Transactions on*, vol. 11, no. 2, pp. 571–583, 2012.

[26] O. Ozel, J. Yang, and S. Ulukus, "Optimal broadcast scheduling for an energy harvesting rechargeable transmitter with a finite capacity battery," *Wireless Communications, IEEE Transactions on*, vol. 11, no. 6, pp. 2193–2203, 2012.

[27] M. A. Antepli, E. Uysal-Biyikoglu, and H. Erkal, "Optimal packet scheduling on an energy harvesting broadcast link," *Selected Areas in Communications, IEEE Journal on*, vol. 29, no. 8, pp. 1721–1731, 2011.

[28] O. Ozel, K. Tutuncuoglu, J. Yang, S. Ulukus, and A. Yener, "Transmission with energy harvesting nodes in fading wireless channels: Optimal policies," *Selected Areas in Communications, IEEE Journal on*, vol. 29, no. 8, pp. 1732–1743, 2011.

[29] P. Mitran, "On optimal online policies in energy harvesting systems for compound poisson energy arrivals," in *Information Theory Proceedings (ISIT), 2012 IEEE International Symposium on*, pp. 960–964, IEEE, 2012.

[30] K. Tutuncuoglu and A. Yener, "Sum-rate optimal power policies for energy harvesting transmitters in an interference channel," *Communications and Networks, Journal of*, vol. 14, no. 2, pp. 151–161, 2012.

[31] C. Huang, R. Zhang, and S. Cui, "Throughput maximization for the gaussian relay channel with energy harvesting constraints," *Selected Areas in Communications, IEEE Journal on*, vol. 31, no. 8, pp. 1469 – 1479, 2013.

[32] D. Gunduz and B. Devillers, "Two-hop communication with energy harvesting," in *Computational Advances in Multi-Sensor Adaptive Processing (CAMSAP), 2011 4th IEEE International Workshop on*, pp. 201–204, IEEE, 2011.

[33] B. Devillers and D. Gunduz, "A general framework for the optimization of energy harvesting communication systems with battery imperfections," *Communications and Networks, Journal of*, vol. 14, no. 2, pp. 130–139, 2012.

[34] K. Tutuncuoglu and A. Yener, "Communicating using an energy harvesting transmitter: Optimum policies under energy storage losses," *arXiv preprint arXiv:1208.6273*, 2012.

[35] T. M. Cover and J. A. Thomas, *Elements of information theory*. John Wiley & Sons, 2012.

[36] F. J. Piera, R. R. Mazumdar, and F. M. Guillemin, "Boundary behavior and product-form stationary distributions of jump diffusions in the orthant with state-dependent reflections," *Advances in Applied Probability*, vol. 40, no. 2, pp. 529–547, 2008.

[37] S. Asmussen, "Applied probability and queues: Stochastic modelling and applied probability," *Applications of Mathematics (New York)*, vol. 51, 2003.

[38] M. B. Khuzani and P. Mitran, "On online energy harvesting in multiple access communication systems," *Information Theory, IEEE Transactions on*, vol. 60, pp. 1883 – 1898, 2014.

[39] R. M. Corless, G. H. Gonnet, D. E. Hare, D. J. Jeffrey, and D. E. Knuth, "On the lambertw function," *Advances in Computational mathematics*, vol. 5, no. 1, pp. 329–359, 1996.

[40] P. Castiglione and G. Matz, "Energy-neutral source-channel coding with battery and memory size constraints," *arXiv preprint arXiv:1309.0239*, 2013.

[41] P. Castiglione, O. Simeone, E. Erkip, and T. Zemen, "Energy management policies for energy-neutral source-channel coding," *Communications, IEEE Transactions on*, vol. 60, pp. 2668 – 2678, 2011.

[42] T. Goblick Jr, "Theoretical limitations on the transmission of data from analog sources," *Information Theory, IEEE Transactions on*, vol. 11, no. 4, pp. 558–567, 1965.

[43] M. Goossens, F. Mittelbach, and A. Samarin, *The LaTeX Companion*. Reading, Massachusetts: Addison-Wesley, 1994.

[44] M. B. Khuzani, H. E. Saffar, E. Alian, and P. Mitran, "On optimal online power policies for energy harvesting with finite-state markov channels," in *Information Theory Proceedings (ISIT), 2013 IEEE International Symposium on*, pp. 1586–1590, IEEE, 2013.

[45] D. Knuth, *The TEXbook*. Reading, Massachusetts: Addison-Wesley, 1986.

[46] L. Lamport, *LATEX — A Document Preparation System*. Reading, Massachusetts: Addison-Wesley, second ed., 1994.

[47] X. Liu, O. Simeone, and E. Erkip, "Energy-efficient sensing and communication of parallel gaussian sources," *Communications, IEEE Transactions on*, vol. 60, no. 12, pp. 3826–3835, 2012.

[48] M. S. Motlagh, M. B. Khuzani, and P. Mitran, "On lossy source-channel transmission in energy harvesting communication systems," in *Information Theory (ISIT), 2014 IEEE International Symposium on*, pp. 1181–1185, IEEE, 2014.

[49] D. Niyato, E. Hossain, M. M. Rashid, and V. K. Bhargava, "Wireless sensor networks with energy harvesting technologies: a game-theoretic approach to optimal energy management," *Wireless Communications, IEEE*, vol. 14, no. 4, pp. 90–96, 2007.

[50] J. A. Stankovic and T. He, "Energy management in sensor networks," *Philosophical Transactions of the Royal Society A: Mathematical, Physical and Engineering Sciences*, vol. 370, no. 1958, pp. 52–67, 2012.

[51] J. Yang and S. Ulukus, "Optimal packet scheduling in a multiple access channel with rechargeable nodes," in *Communications (ICC), 2011 IEEE International Conference on*, pp. 1–5, IEEE, 2011.